SHEAR STRENGTH TESTING OF ROCK FRACTURES UNDER CONSTANT NORMAL LOAD AND CONSTANT NORMAL STIFFNESS AS AFFECTED BY DISPLACEMENT RATES

Pinid Meemun

A Thesis Submitted in Partial Fulfillment of the Requirements for the Degree of Master of Engineering in Geotechnology

Suranaree University of Technology

Academic Year 2014

การทดสอบกำลังเฉือนของรอยแตกในหินแบบความเค้นตั้งฉากคงที่และแบบการเคลื่อนตัวในแนวตั้งฉากคงที่ที่มีผลกระทบจากอัตราการเคลื่อนตัว

นายพินิจ มีมั่น

วิทยานิพนธ์นี้เป็นส่วนหนึ่งของการศึกษาตามหลักสูตรปริญญาวิศวกรรมศาสตรมหาบัณฑิต
สาขาวิชาเทคโนโลยีธรณี
มหาวิทยาลัยเทคโนโลยีสุรนารี
ปีการศึกษา 2557

SHEAR STRENGTH TESTING OF ROCK FRACTURES UNDER CONSTANT NORMAL LOAD AND CONSTANT NORMAL STIFFNESS AS AFFECTED BY DISPLACEMENT RATES

Suranaree University of Technology has approved this thesis submitted in partial fulfillment of the requirements for a Master's Degree.

Thesis Examining Committee

_____

(Dr. Prachya Tepnarong)

Chairperson

_____

(Prof. Dr. Kittitep Fuenkajorn)

Member (Thesis Advisor)

_____

(Dr. Decho Phueakphum)

Member

_____ _____

(Prof. Dr. Sukit Limpijumnong) (Assoc. Prof. Flt. Lt. Dr. Kontorn Chamniprasart)

Vice Rector for Academic Affairs and Innovation

Dean of Institute of Engineering

พินิจ มีมั่น : การทดสอบกำลังเฉือนของรอยแตกในหินแบบความเค้นตั้งฉากคงที่และแบบการเคลื่อนตัวในแนวตั้งฉากคงที่ที่มีผลกระทบจากอัตราการเคลื่อนตัว (SHEAR STRENGTH TESTING OF ROCK FRACTURES UNDER CONSTANT NORMAL LOAD AND CONSTANT NORMAL STIFFNESS AS AFFECTED BY DISPLACEMENT RATES) อาจารย์ที่ปรึกษา : ศาสตราจารย์ ดร.กิตติเทพ เฟื่องขจร, 55 หน้า.

วัตถุประสงค์ของงานวิจัยเพื่อศึกษาหากำลังเฉือนของรอยแตกในหินภายใต้สภาวะแบบความเค้นตั้งฉากคงที่และแบบการเคลื่อนตัวในแนวตั้งฉากคงที่ที่มีผลกระทบจากอัตราการเคลื่อนตัว โดยหินอ่อนที่ใช้ในการทดสอบเป็นหินจากชุดสระบุรี ตัวอย่างหินที่ใช้ในการทดสอบมีขนาดเท่ากับ 100x100x180 ลูกบาศก์มิลลิเมตร พื้นที่หน้าตัดของรอยแตกที่ใช้ในการทดสอบมีขนาดเท่ากับ 90x100 ตารางมิลลิเมตร รอยแตกของตัวอย่างหินทำการจำลองขึ้นในห้องปฏิบัติการโดยวิธีการให้แรงกดแบบแนวเส้นเพื่อให้เกิดแรงดึงในตัวอย่างหิน ทำการทดสอบกำลังเฉือนแบบตรงโดยให้แรงกดตั้งฉากกับรอยแตกคงที่ผันแปรจาก 0.5, 1.0, 1.5 และ 2.0 เมกกะปาสคาลและการทดสอบแบบการเคลื่อนที่ในแนวตั้งฉากคงที่ ใช้อัตราการเฉือนผันแปรจาก 10^{-4}, 10^{-3}, 10^{-2} และ 10^{-1} มิลลิเมตรต่อวินาที สำหรับแบบความเค้นตั้งฉากคงที่และแบบการเคลื่อนตัวในแนวตั้งฉากคงที่ที่มีผลกระทบจากอัตราการเคลื่อนตัว ผลการวิจัยที่ได้จากห้องปฏิบัติการสามารถตรวจสอบในความสัมพันธ์ของ แบบความเค้นตั้งฉากคงที่ แบบการเคลื่อนตัวในแนวตั้งฉากคงที่ ความเครียด และอัตราการเคลื่อนตัวในแนวกำลังเฉือน และสามารถนำความสัมพันธ์จากข้อมูลดังกล่าว มาใช้ในงานวิเคราะห์ ประเมินเสถียรภาพของโครงสร้างในงานวิศวกรรม และงานโครงสร้างทางธรณีวิทยา ตัวอย่างเช่น งานอุโมงค์ งานเหมืองใต้ดิน และงานโครงสร้างฐานรากของเขื่อน เป็นต้น

สาขาวิชา เทคโนโลยีธรณี ลายมือชื่อนักศึกษา _____

ปีการศึกษา 2557 ลายมือชื่ออาจารย์ที่ปรึกษา_____

PINID MEEMUN : SHEAR STRENGTH TESTING OF ROCK FRACTURES UNDER CONSTANT NORMAL LOAD AND CONSTANT NORMAL STIFFNESS AS AFFECTED BY DISPLACEMENT RATES. THESIS ADVISOR : PROF. KITTITEP FUENKAJORN, Ph.D., P.E., 55 PP

ROCK JOINT/ SHEAR STRENGTH/ CONSTANT NORMAL LOAD/ CONSTANT NORMAL STIFFNESS

The objective of this study is to determine shear strengths of factures under constant normal loads (CNL) and constant normal stiffness (CNS) conditions as affected by displacement rates. The rock specimens are prepared from Saraburi marble having nominal dimensions of 100×100×180 mm^3. The fracture area is about 100×90 mm^2. The fractures are artificially made in the laboratory by tension inducing method. The direct shear test is performed with constant normal stresses at 0.5, 1.0, 1.5 and 2.0 MPa for CNL and CNS test conditions. This study is using triaxial loading frame. Applied shear velocity varies are 10^{-4}, 10^{-3}, 10^{-2} and 10^{-1} mm/s. The results from laboratory measurements in terms of constant normal load, constant normal stiffness, stress states and shear displacement are compared. Similarity and discrepancies are identified. Such relation is useful in the stability analysis of engineering structures on and in geologic media, such as tunnels, underground mines and dam foundations.

School of Geotechnology Student's Signature

Academic Year 2014 Advisor's Signature

ACKNOWLEDGMENTS

I wish to acknowledge the funding supported by Suranaree University of Technology (SUT) who has provided funding for this research.

I would like to express my sincere thanks to Prof. Dr. Kittitep Fuenkajorn for his valuable guidance and efficient supervision. I appreciate his strong support, encouragement, suggestions and comments during the research period. My heartiness thanks to Dr. Prachya Tepnarong and Dr. Decho Phueakphum for their constructive advice, valuable suggestions and comments on my research works as thesis committee members. Grateful thanks are given to all staffs of Geomechanics Research Unit, Institute of Engineering who supported my work.

Finally, I would like to thank beloved parents for their love, support and encouragement.

Pinid Meemun

TABLE OF CONTENTS

Page

TABLE OF CONTENTS (Continued)

Page

TABLE OF CONTENTS (Continued)

Page

TABLE OF CONTENTS (Continued)

Page

LIST OF TABLES

Table **Page**

LIST OF FIGURES

Figure **Page**

LIST OF FIGURES (Continued)

Figure **Page**

LIST OF FIGURES (Continued)

Figure **Page**

SYMBOLS AND ABBREVIATIONS

β	=	Empirical constant for equation (6.2)
χ	=	Empirical constant for equation (6.2)
κ	=	Empirical constant for equation (6.3)
λ	=	Empirical constant for equation (6.3)
ASTM	=	American Society for Testing and Materials
c	=	Cohesion
CNL	=	Constant normal load
CNS	=	Constant normal stiffness
d_n	=	Normal displacement
DS	=	Direct shear test (in Table 3.1, 3.2)
d_s	=	Shear displacement
DSM	=	Double shear model
JCS	=	Joint compressive strength
JMC	=	Joint matching coefficient
JRC	=	Joint roughness coefficient
K_s	=	Joint shear stiffness
LVDT	=	Linear volte displacement transformer
MB	=	Marble (in Table 3.1, 3.2)
$R_{L,P}$	=	Parallel profile roughness parameter
$R_{L,T}$	=	Trisector profile roughness parameter

SYMBOLS AND ABBREVIATIONS (Continued)

R_s	=	Surface roughness parameter
H–B	=	Hoek-Brown
M–X	=	Mohr Coulomb
$\delta d_s/\delta t$	=	Shear displacement rate
ϕ	=	Friction angle
σ_n	=	Initial normal stress
τ	=	Shear stress

CHAPTER I

INTRODUCTION

1.1 Background and rationale

The presence of joints in the rock can affect its mechanical behavior, depending on the underground conditions. If the dilation of the rock joint during shearing is constrained or partially constrained, an increase in the normal stress over the shear plane will occur, this substantially increases the shear resistance. An underground excavation is potentially unstable rock blocks are constrained between two parallel dilatant rocks (Indraratna et al., 1999). The sliding of such blocks inevitably increases the normal stress, and also, dilation becomes significant if the joint surfaces are rough. Tests conducted under constant normal load (CNL) condition yield shear strengths that are too low for such practical situations. Another situation where the normal changes during shearing is the earthquake shaking of slope, where the direction of shearing and the magnitude of normal load on any potential sliding plane are variable during shaking. In general, the CNL condition is only realistic for shearing of planar interfaces, where the normal stress applied to the shear plane remains relatively constant, such as in the case of rock slope stability problems. For situations as illustrated, the development of shear resistance is a function of constant normal stiffness, and the use of CNL test results for such cases leads to underestimated shear strengths.

1.2 Research objectives of this study

The objective of this study is to determine shear strengths of factures under constant normal loads (CNL) and constant normal stiffness (CNS) conditions, as affected by displacement rates. The rock specimens are prepared from the Saraburi marble having nominal dimensions of 100×100×180 mm^3. The fracture area is about 100×90 mm^2. The fractures are artificially made in the laboratory by tension inducing method. The direct shear test is performed with constant normal stresses at 0.5, 1.0, 1.5 and 2.0 MPa and using triaxial loading frame. The applied shear velocities are 10^{-4}, 10^{-3}, 10^{-2} and 10^{-1} mm/s. The results from laboratory measurements in terms of constant normal load, constant normal stiffness, stress states and shear displacement are compared. Similarity and discrepancies are identified. Such relation is useful in the stability analysis of engineering structures on and in geologic media, such as tunnels, underground mines and dam foundations.

1.3 Research methodology

The research methodology shown in Figure 1.1 comprises 6 steps; including literature review, sample preparation, laboratory testing, comparisons, discussions, conclusions and thesis writing.

1.3.1 Literature review

Literature review is carried out to study the previous researches on dependent the effect of intermediate principal stress until true triaxial shear tests. The sources of information are from text books, journals, technical reports and conference papers. A summary of the literature review is given in the thesis.

1.3.2 Sample preparation

Specimen preparation is carried out in the laboratory at Suranaree University of Technology. The rock specimens used in this research are Saraburi marble prepared to obtain rectangular block specimens with the nominal dimensions of 100×100×230 mm^3 for fracture surface with an area of 100×90 mm^2, and 100×100×180 mm^3 for fracture surface with an area of 100×90 mm^2. The fractures are artificially made in the laboratory by tension-induced method as shown in Figure 1.2.

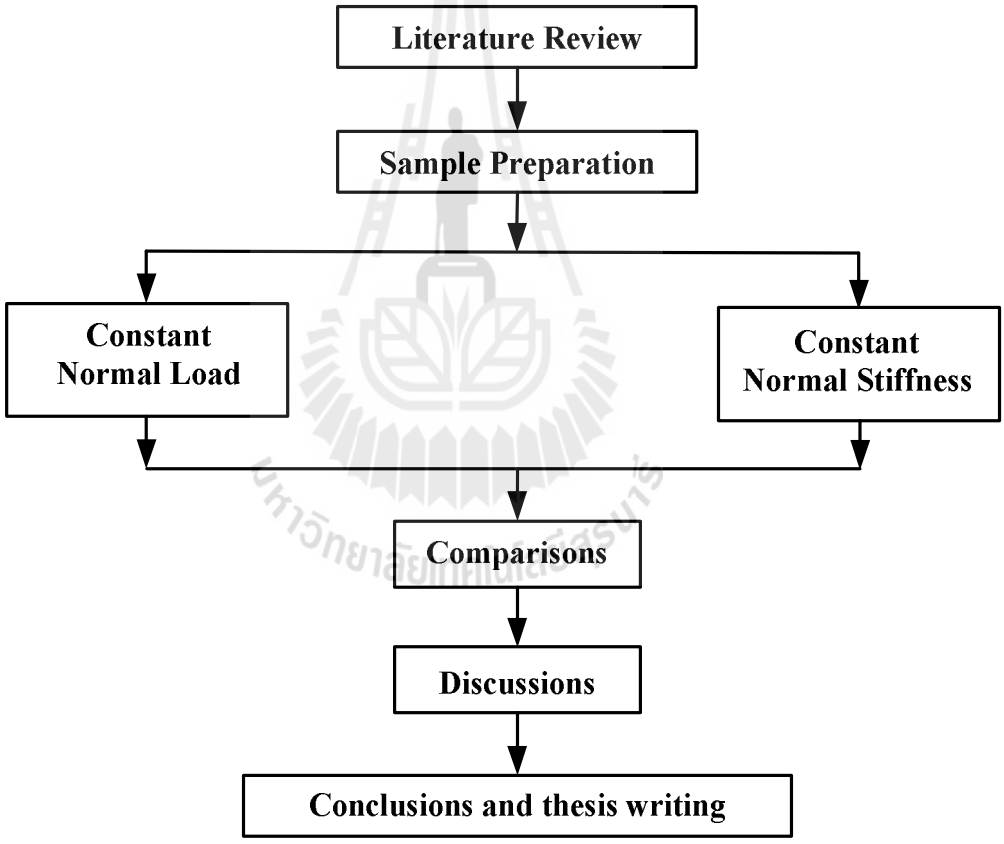

Figure 1.1 The research methodology.

1.3.3 Laboratory testing

The true triaxial load frame (Fuenkajorn and komenthammasopon, 2014) is used to determine the shear strength by applying true triaxial stress to the specimens and to develop sliding criteria of fracture in marble. The direct shear test is performed with initial normal stresses at 0.5, 1.0, 1.5 and 2.0 MPa for CNL and CNS test conditions. The applied shear displacement rates are 10^{-4} to 10^{-1} mm/s. The neoprene sheets are used to minimize the friction at all interfaces between the loading plate and the rock surface.

1.3.4 Comparisons

The test results are shown as function of peak shear strength, friction angle and cohesion comparisons between CNL and CNS test conditions.

1.3.5 Discussions

The research results are discussed and comparison with other researches performed elsewhere.

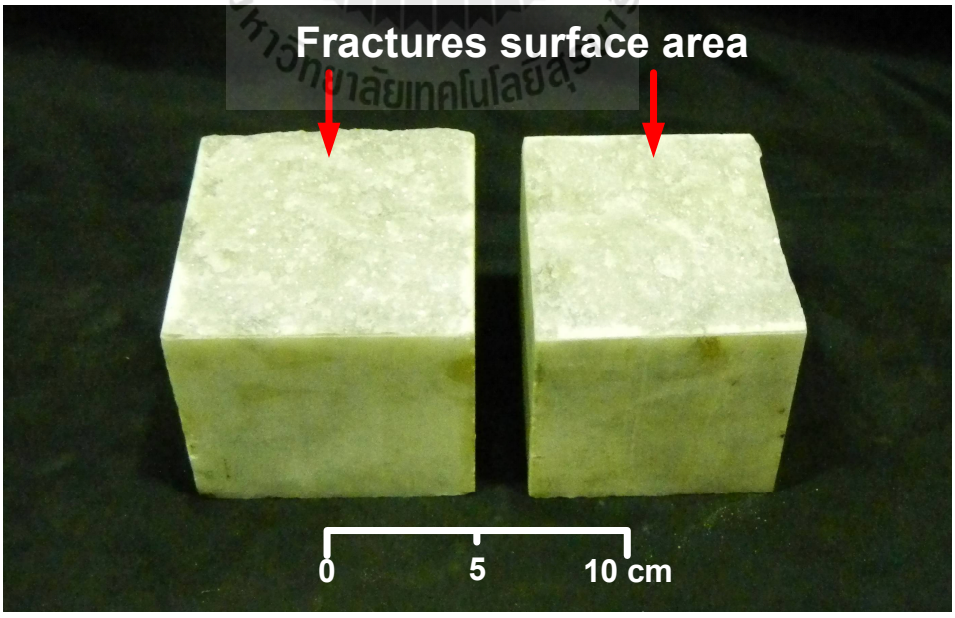

Figure 1.2 The fractures surface area.

1.3.6 Conclusions and recommendations for future studies thesis writing

The test method and results are decussated and concluded. The recommendations for future studies are given.

1.3.7 Thesis writing

All research activities, methods, and results are documented and complied in the thesis. The research or findings are published in the conference proceedings or journals.

1.4 Scope and limitations

The scope and limitations of the research include as follows.

1. Laboratory experiments are conducted on specimens prepared from Saraburi marble.
2. Direct shear tests are performed with constant normal stresses at 4 levels (0.5, 1.0, 1.5, and 2.0 MPa) using a triaxial loading frame.
3. Applied shear displacements vary from 10^{-4}, 10^{-3}, 10^{-2} and 10^{-1} mm/s.
4. All tested fractures are artificially made in the laboratory by tension induced method.
5. The tests use fracture areas of 100 x 90 mm^2.
6. Up to 32 samples are tested.
7. All tests are conducted under ambient temperature.

1.5 Thesis contents

Chapter I describes the objectives, the problems and rationale, and the methodology of the research. **Chapter II** summarizes results of the literature review on

CNL and CNS test conditions. **Chapter III** describes the saraburi marble sample collections and preparations. **Chapter IV** describes the laboratory testing and presents the initial result obtained for the laboratory testing. **Chapter V** presents the test results and the comparison between CNL and CNS test conditions. **Chapter VI** concludes the research result and provides recommendations for future research studies.

CHAPTER II

LITERATURE REVIEW

2.1 Introduction

This chapter summarizes the results of literature review carried out to improve an understanding the joint shear strengths under constant normal load and constant normal stiffness test conditions, the topics reviewed here include the behavior of rock joint under constant normal load and constant normal stiffness test conditions, effect of shear strength, cohesions and friction angle on rock fracture, numerical model and shear strength criterion.

2.2 Literature reviews

2.2.1. Constant normal load and constant normal stiffness test conditions

Indraratna et al. (1997) study the shear behavior of synthetic soft rock joints (regular saw-tooth) in the laboratory under constant normal stiffness condition. A large-scale shear apparatus is designed and constructed which can test joints under both CNL and CNS conditions. It is observed that CNL condition overestimates joint dilation compared to CNS condition and thereby, underestimates the peak shear stress of joints. Plot of shear stress against normal stress, shows that a bilinear shear strength envelope is suitable for soft rock joints subjected to CNL conditions, while linear or bilinear envelopes are acceptable for CNS testing depending on the asperity

angles. The shear behavior of infilling joints is also investigated under CNS conditions, and it is found that a very small thickness of bentonite infill reduced the shear strength significantly. The shear strength of joints almost approached that of pure infill, when the infill thickness to asperity height ratio reaches to 1.60.

Direct shear testing (e.g., ASTM D5607-08) has widely been used to determine the peak and residual strengths of the rock fractures. Its test configurations however pose some disadvantages that the magnitudes of the applied normal stress are limited by the uniaxial compressive strength of the rock and that the fractures are sheared under unconfined conditions. The triaxial shear testing (Brady and Brown, 2006; Jaeger et al., 2007) has been developed to simulate the frictional resistance of rock fractures under confinements.

Rim et al. (2005) studied the shear behavior of rock discontinuities is critical for understanding mechanical behavior of rock mass. Direct shear tests on the rock discontinuities can be divided into two types: constant normal load direct shear test, where the normal load on the discontinuity remains constant during the shear test, and constant normal stiffness direct shear test, where the normal load varies according to the normal dilation.

The CNL direct shear test can be applied to predict the shear behavior of a rock slope, where the normal load on the discontinuities is relatively small and constant. The CNL direct shear test, however, has been used also for many underground rock joint shear tests, just because of neglect of the difference between rock slope and underground.

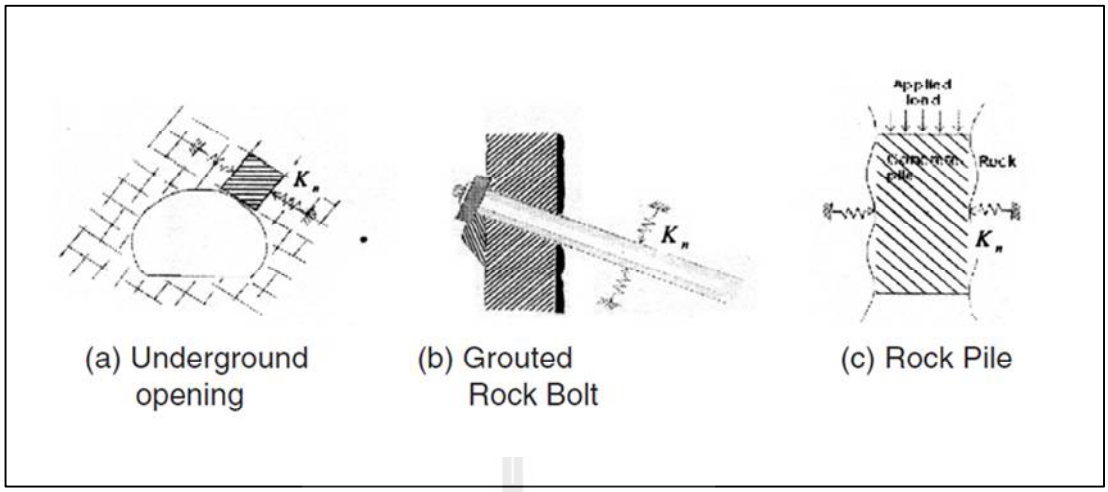

Figure 2.1 The examples of the constant normal stiffness condition (Mouchaorab et al., 1994)

For the underground rock joints as shown in Figure 2.1, the normal stress on the rock joint is determined by normal stiffness and normal displacement of the joint. In CNS direct shear test, the constant normal stiffness can be obtained by inserting a spring between a load frame and a joint sample or by adopting a servo-controlled shear machine. Of course, the servo controlled machine is more versatile and provides more precise results.

2.2.2. Factors affecting the joint shear strength

Babanouri et al. (2011) stated that although many researchers have studied the normal and shear behavior of fractures under stresses, the over-consolidation effect on the slip/shear behavior of discontinuities has not been considered. The over-consolidation behavior of non-planar rock fractures should be considered when deposition-consolidation-erosion (or excavation) sequences occur. Plaster replicas of representative natural rock joint surfaces are prepared for this

study. In this case, the surface roughness and other geometrical properties remain constant during the laboratory direct shear tests. It is observed that the shear strength within a large range of roughness, joint wall strength and normal stress values significantly increases with increasing over-consolidation ratio. According to the test results, a new model is developed as an extended form of Barton's shear failure criterion for rock joints. This model considers the effect of various paths of normal loading/unloading before shearing and over-consolidation ratio (OCR) in a fracture. A new joint over-closure (JOC) parameter is also introduced as the ratio of closure in over-closed to normally closed conditions.

2.2.3. Numerical model

Bahaaddini et al. (2013) study the shear behavior of rock joints using the discrete element code PFC2D. In PFC, the intact rock is represented by an assembly of separate particles bonded together where the damage process is represented by the breakage of these bonds. Traditionally, joints have been modeled in PFC by removing the bonds between particles. This approach however is not able to reproduce the sliding behavior of joints and also results in an unrealistic increase of shear strength and dilation angle due to the inherent micro-scale roughness of the joint surface. Modeling of joints in PFC is improved by the emergence of the smooth joint model. In this model, slip surfaces are applied to contacts between particles lying on the opposite sides of a joint plane. Results from the current study show that this method suffers from particle interlocking which takes place at shear displacements greater than the minimum diameter of the particles. To overcome this problem, a new shear box genesis approach is proposed. The ability of the new method in

reproducing the shear behavior of rock joints is investigated by undertaking direct shear tests on saw-tooth triangular joints with base angles of 15, 25and 35and the standard joint roughness coefficient profiles. A good agreement is found between the results of the numerical models and the Patton, Ladanyi and Archambault and Barton and Choubey models. The proposed model also has the ability to track the damage evolution during the shearing process in the form of tensile and shear fracturing of rock asperities.

Park and Song (2013) use a numerical method to determine the contact areas of a rock joint under normal and shear loads. The method requires only three-dimensional surface coordinates at the initial stage before shearing, while some disparate materials are inserted between the joint surfaces or particular equipment are adopted for measurement of the contact areas during the test in other conventional methods. The joint surface is modeled as a group of triangular planes, and the contact condition of each plane is examined by calculating the relative displacements of both surfaces from their initial locations. To verify the method, a direct shear test on a rock joint is simulated using a bonded particle model in a discrete element code. The locations of the contact areas observed in the simulation showed good agreement with those determined using the proposed method. To apply these techniques, the experimental results of shear tests on replicas of rock joints are analyzed for the location, size and micro-slope angle of contact areas according to the following shearing stages: pre- peak, peak, post-peak and residual. The locations of the contact areas are closely correlated with the distribution of the micro-slope angle, which indicates that the joint roughness should be qualified with respect to the shear

direction and the corresponding contact area. Additionally, the proposed method is applied to estimation of the distribution of aperture size within a rock joint.

Hongwai et al. (2010) use Double Shear Model (DSM) in a numerical simulation on bolted rock joint shearing performance. An entire bolt deformed as the letter "U" under a shear load between two joints. Near the bolt-joint intersection, the bolt partly deformed as the letter "Z". There are two critical points along the bolt: one is at the bolt-joint intersection with zero bending moment and the other at the maximum bending moment (plastic hinge) with zero shear stress. The blocks on two sides slid along the bolt as it deformed. A separation area is found between the two joint contact surfaces of the middle rock block and sided block. This area of separation is related to bolt diameter and external forces. They assume that this area is related to the work of external forces. Further research is needed.

2.2.4. Shear strength criterion

Kusumi et al. (1997) state that a new formulation of shear strength for irregular rock joints by Ladanyi's shear strength criterion (1970) is only applied to the regular triangular joints. The purpose of this study is the proposal of a new shear strength criterion which is applied to irregular joints. First of all, the appropriate estimation method of irregular joint profiles must be quantitatively estimated. The artificial plaster specimens have four different JRC profiles, and the sandstone specimens including the irregular joint are applied on the direct shear test. The measurement and analysis of joint surface profile for each specimen using laser profilometer have conducted. As the results, the new experimental equations which exactly represent the shear strength parameters included in Ladanyi's shear strength

criterion is proposed, and it is recognized that this new experimental equations can be applied for the rock specimens having the irregular joint.

Kenkhunthod and Fuenkajorn (2010) study the influence of loading rate on deformability and compressive strength of three Thai sandstones. Uniaxial and triaxial compressive strength tests have been performed using a polyaxial load frame to assess the influence of loading rate on the strength and deformability of three Thai sandstones. The applied axial stresses are controlled at constant rates of 0.001, 0.01, 0.1, 1.0 and 10 MPa/s. The confining pressures are maintained constant at 0, 3, 7 and 12 MPa. The sandstone strengths and elastic moduli tend to increase exponentially with the loading rates. The effects seem to be independent of the confining pressures. An empirical loading rate dependent formulation of both deformability and shear strength is developed for the elastic and isotropic rocks. It is based on the assumption of constant distortional strain energy of the rock at failure under a given mean normal stress. The proposed multiaxial criterion well describes the sandstone strengths within the range of the loading rates used here. It seems reasonable that the derived loading rate dependent equations for deformability and shear strength are transferable to similar brittle isotropic intact rocks.

Zhao (1997) states that the JRC-JCS model (Barton's JRC-JCS shear strength criterion 1976) tends to over-predict the shear strength for those natural joints with less matched surfaces. To overcome this shortcoming, a new JRC-JMC shear strength criterion is proposed in order to include the effects of both joint surface roughness and joint matching, in the form of $\tau = \sigma_n \cdot \tan [JRC \cdot JMC \cdot \log10 (JCS/\sigma_n) + \phi_r]$. The new JRC-JMC model provides appropriate fining of the shear test results and

gives a better interpretation and prediction, particularly for natural joints that do not have perfectly matched surfaces.

Grasselli and Egger (2002) propose a new constitutive criterion, relating stress and displacements, to model the shear resistance of joints under constant normal load conditions. It is based on an empirical description of the surface, and on the results from more than 50 constant normal-load direct-shear tests performed on replicas of tensile joints and on induced tensile fractures for seven rock types. This constitutive model is able to describe experimental shear tests conducted in the laboratory. Moreover, the parameters required in the model can be easily measured through standard laboratory tests. The proposed criterion is also used to estimate the joint roughness coefficient (JRC) value. The predicting values are successfully correlated with JRC values obtained by back analysis of shear tests.

Maksimovic (1996) proposes a non -linear failure envelope of hyperbolic type in terms of effective stresses for rock discontinuities is described by a simple three parameter expression, which contains the basic angle of friction, the roughness angle and the median angle pressure. The components of friction, dilation and breakage of asperities are derived. The proposed expressions are related to the widely used, failure law, of a logarithmic type proposed by Barton and the simple correspondence of ‘two sets of parameters derived. Comparison with the power type expressions und possibilities for conversion is presented. Several experimental results are used for verification of the proposed relations. It is shown that the proposed hyperbolic relation has significant advantages.

Barton (2013) proposes non-linear shear strength envelopes for intact rock and for (non-planar) rock joints. Traditional shear test interpretation and

numerical modeling in rock mechanics has ignored this for a long time. The non-linear Hoek–Brown (H-B) criterion for intact rock is eventually adopted, and many have also used the non-linear shear strength criterion for rock joints, using the Barton and Choubey wall-roughness and wall- strength parameters JRC (joint roughness coefficient) and JCS (joint compressive strength). Non-linearity is also the rule for the peak shear strength of rock fill. It is therefore somewhat remarkable why so many are still wedded to the '$c + \sigma_n \tan\varphi$' linear strength envelope format. Simplicity is hardly a sub statute for reality. Illustrates a series of simple strength criteria that predate H-B, and that are distinctly different from Mohr–Coulomb (M-C), due to their non- linearity. The actual shear strength of rock masses, meaning the prior failure of the intact bridge sand then shear on the fracture sand joints at larger strains, is shown in Figure 2.2 (units of σ_1 and σ_2 are in MPa).

Lee et al. (2006) study the shear strength of jointed rock to identify the most important factors for design and construction of the underground structures in rock. It is greatly influenced by effective normal stress, joint wall compressive strength and joint roughness. Since joint roughness has considerable influence on the shear strength of jointed rock, many studies have been conducted to get a quantitative joint roughness value. Until now, joint roughness coefficient (JRC) proposed by Barton has been prevalently used as a rock joint roughness parameter in spite of its inherent disadvantages.

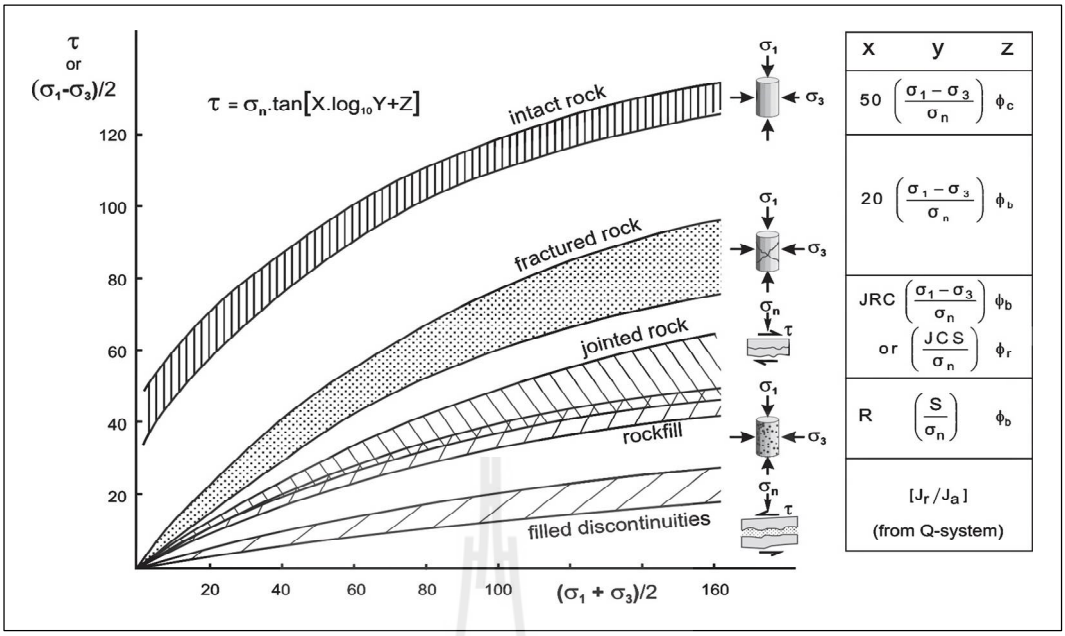

Figure 2.2 The simple empiricism, sometimes based on hundreds of test samples, suggested these simple ways to express peak shear strength (Barton., 1976)

A quantification of rock joint roughness is performed using the parallel profile roughness parameter, $R_{L,P}$, trisector profile roughness parameter, $R_{L,T}$ and surface roughness parameter, R_s. A total of 29 rock core joints are investigated. It is observed that the values of R_s are in the range of about 1.01–1.08 and $R_{L,T}$ and $R_{L,P}$ exist in the range of 1.01–1.04 and 1.01–1.05, respectively and appropriately represent the degree of joint roughness. It is noted that at least a two-digit precision in the roughness value needs to be calculated due to the parameter's sensitivity to roughness.

Based on the quantification of joint surface roughness, joint shear tests are performed with the portable shear box. The relationship between joint surface roughness and joint shear strength is investigated. As expected, the test performed using higher joint roughness results in higher peak strength as shown in Figure 2.3. It

is found that for the smooth joint roughness, sliding of the rock cores is the principal shear mechanism; however, the breakage of roughness from the rock cores is inferred for rougher joint roughness.

A new peak shear strength criterion for rock joints is derived from these results. It is the one that substitutes only the roughness parameter, JRC in Barton's equation with surface roughness parameter, R_s. Using the regression curve between JRC and R_s, the new peak shear strength equation for rock joint is derived. The equation has considerable credibility and originality in that it is obtained from laboratory tests and expressed with quantified parameters as shown in equation (1).

$$\tau_f = \sigma_n \text{ x } \tan (\phi_b + (169.2 \text{ x } \ln(R_s) + 9.1) \log (\frac{\sigma_d}{\sigma_n})) \quad (2.1)$$

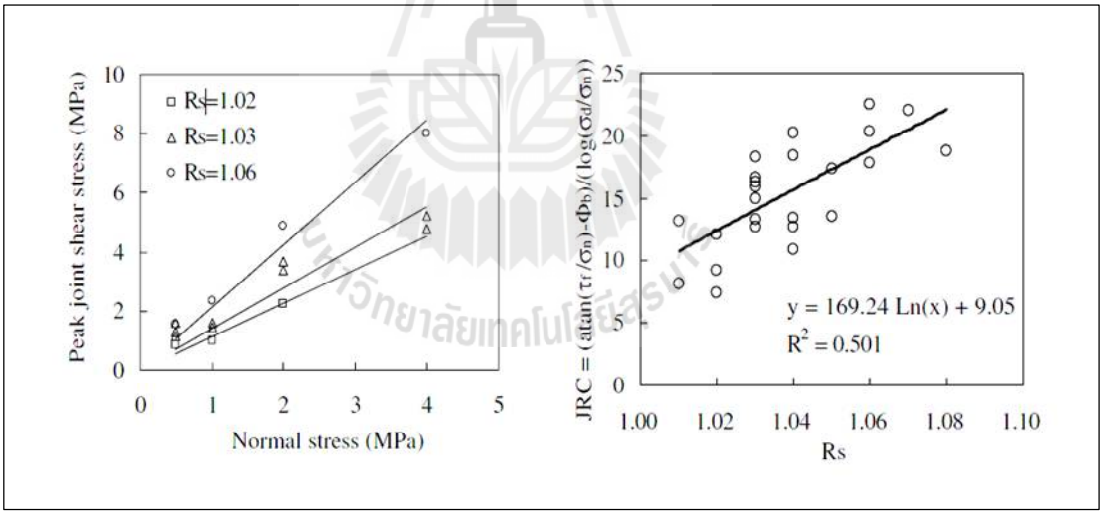

Figure 2.3 The results of higher joint roughness in higher peak strength (Lee et al.,2006)

2.2.5. Shear velocity of rock joint

Jafari et al. (2003) study the effects of shearing velocity on shear strength, some monotonic tests are performed in different ranges of axial displacement in 4 MPa confining pressure from 0.05 to 0.4 mm/s. The differences between the curves can be related to the effects of shear velocity on second-order asperities, as the total applied displacement is limited. It is observed that shear strength reduces with increasing shear velocity, approaching the same values for the peak and residual strength as shown Figure 2.4.

Li et al (2012) study shear test under normal stresses of 1, 2 and 4MPa, and shear velocity of 0.5 mm/min. During the CNL tests, the normal stress is maintained constant, consequently, the shear stress increases linearly to reach a maximum (shear strength) and decreases to the residual strength. The slope of the increasing portion of the curve is the shear stiffness k_s of the fracture. The peak shear stress increases proportionally with the normal stress as shown in Figure 2.5. The normal displacement increases fast in the initial stage of shear, then continues to increase but with smaller gradient as shown in Figure 2.6. The dilation of fracture is restricted under larger normal stress.

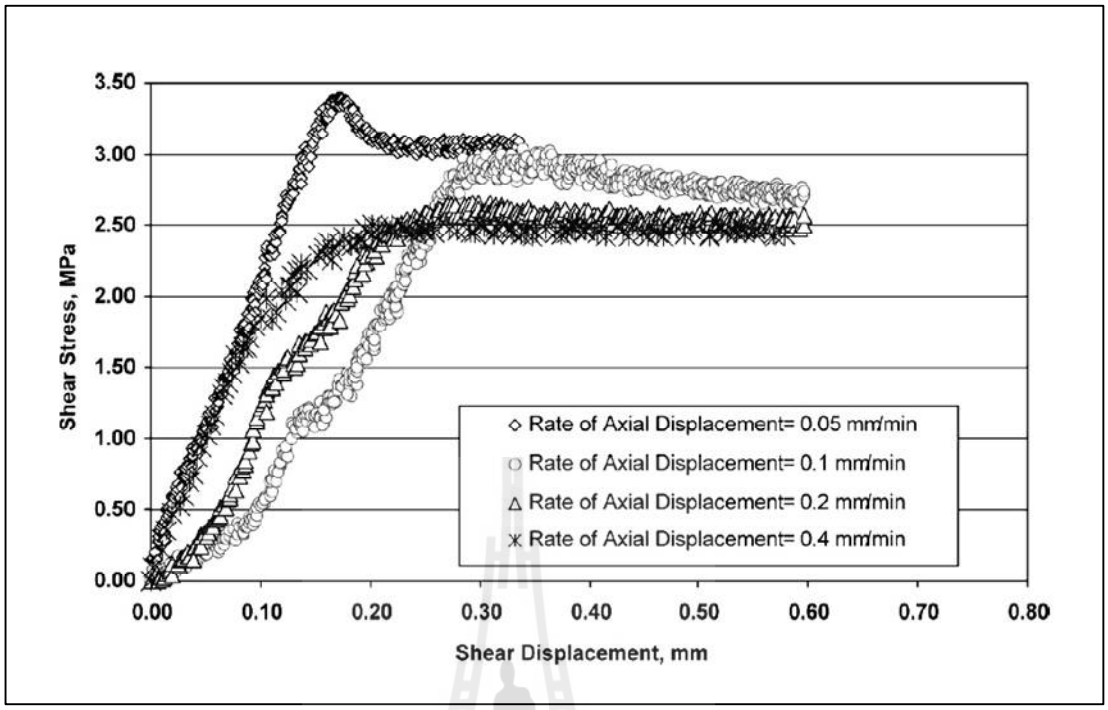

Figure 2.4 The shear stress and shear displacement curve of different rates (Jafari et al., 2003)

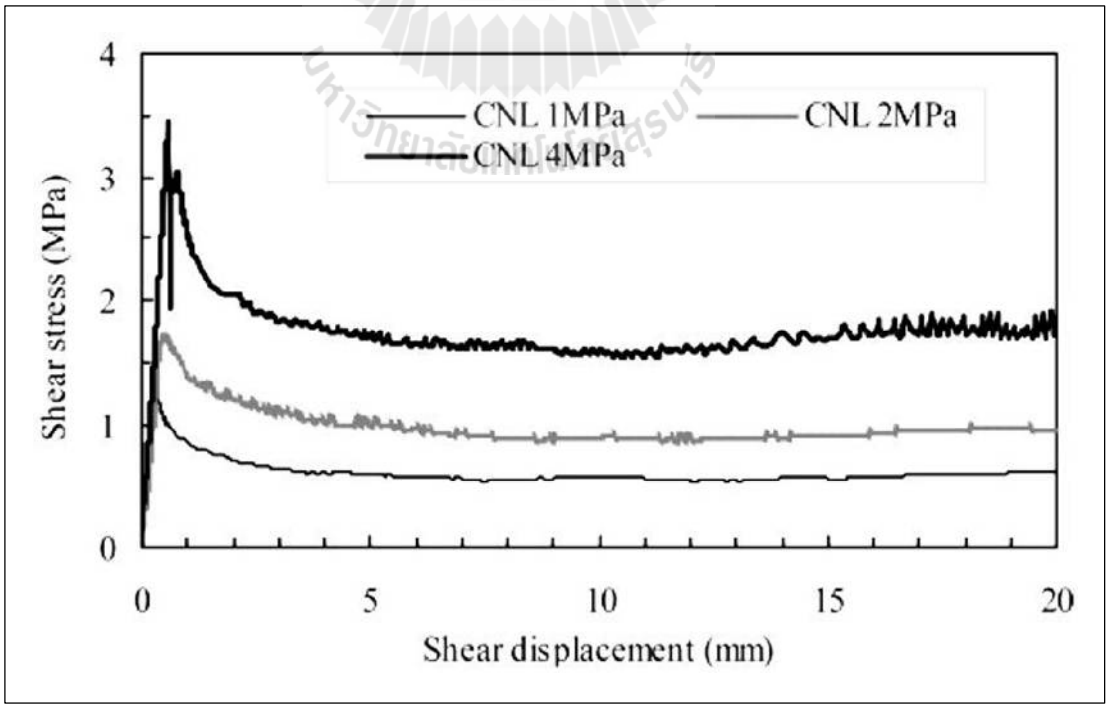

Figure 2.5 The relations between shear stress and shear displacement (Li et al., 2012)

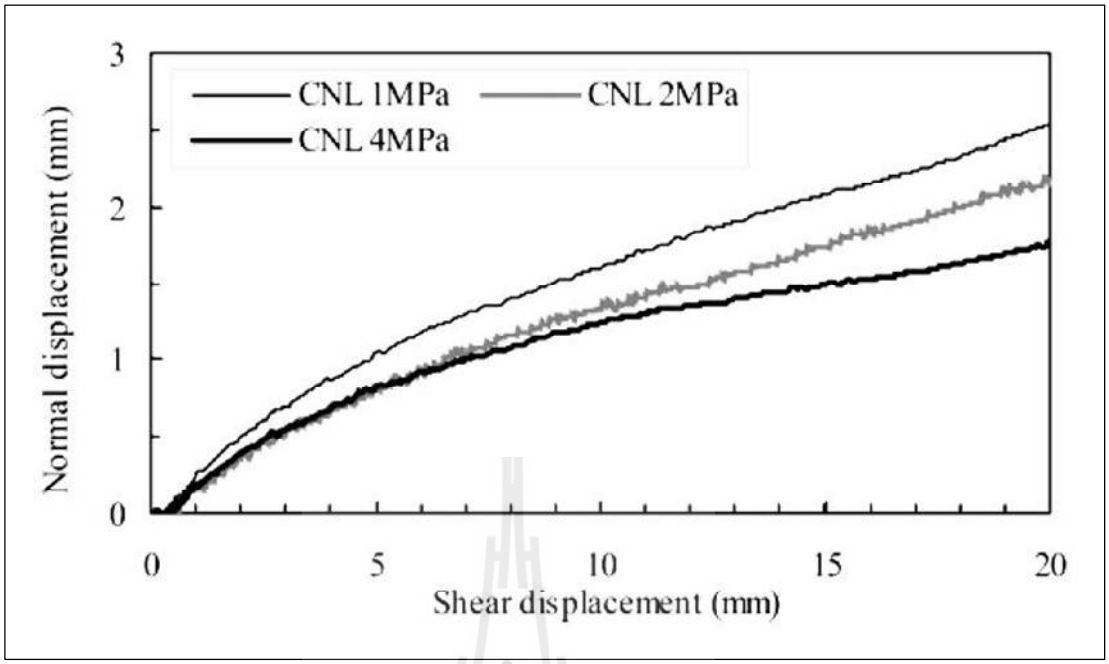

Figure 2.6 The relations between normal displacement and shear displacement (Li et al., 2012)

CHAPTER III

SAMPLE PREPARATION

3.1 Introduction

This chapter describes the rock sample preparation. The rock samples include Saraburi marble (Figure 3.1). These rocks have significant impacts on stability of many engineering structures constructed in region (slope embankments, underground mines and tunnels). They are selected here due to their uniform texture and availability.

3.2 Sample preparation

Thirty-two specimens are prepared for each rock type. The sample preparation is carried out in the laboratory at the Suranaree University of Technology. Specimens for shear test are prepared to have fractures area of about 100×90 square millimeters as show in Table 3.1 for constant normal load test and in Table 3.2 for constant normal stiffness test. The fractures are artificially made in the laboratory by tension inducing in 100×100×180mm^3. Samples comprise2 blocks. Each block has a dimension of 100×100×90 mm^3. The fractures are artificially made in the laboratory by tension-induced method as shown in Figure 3.2.

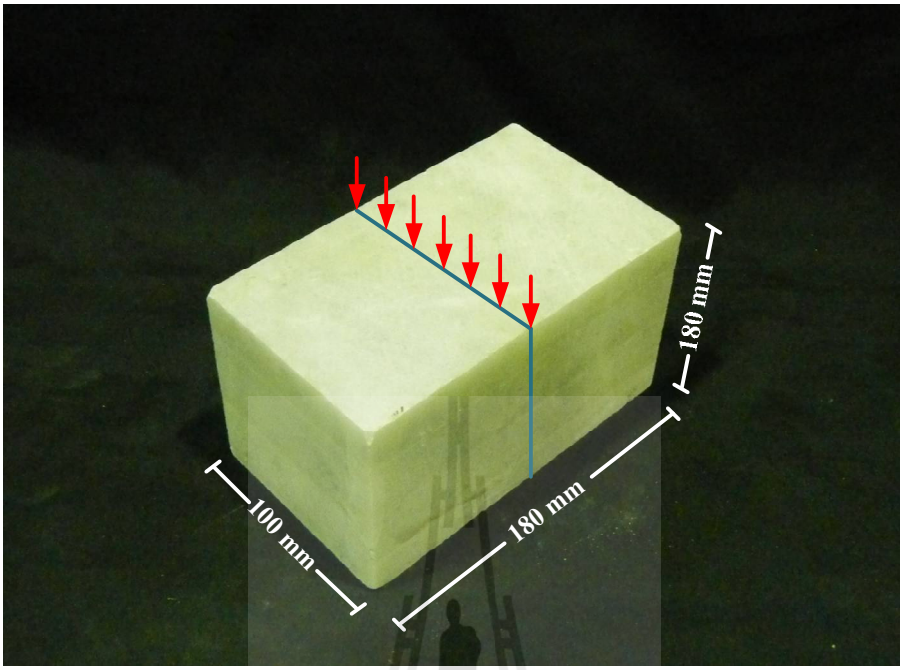

(a) Some rock specimen for preparation.

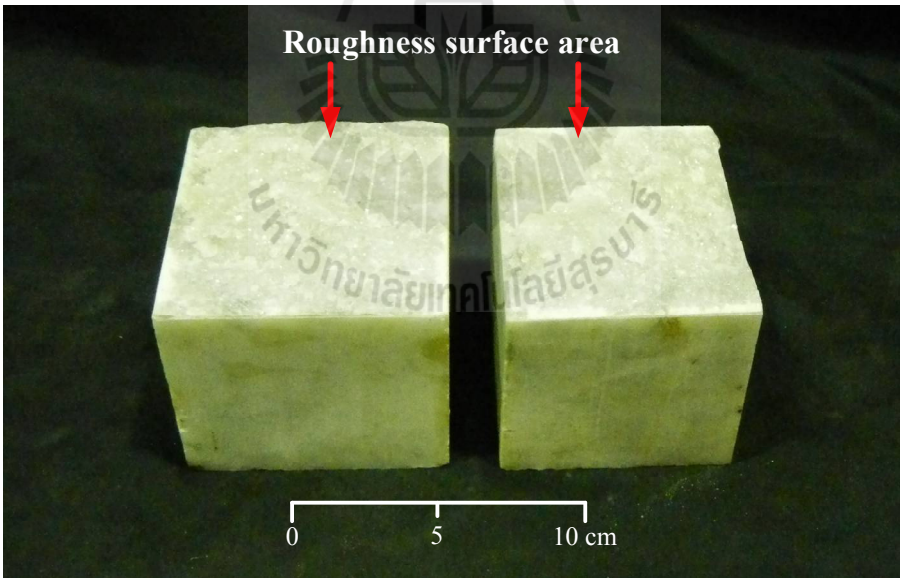

(b) Roughness surface area for shear test.

Figure 3.1 (a)Some rock specimenfor preparation, (b) Roughness surface area for shear test.

Table 3.1 The sample dimensions for constant normal load test.

Sample No.	Length (mm)	Width (mm)	Shear area (mm^2)	$\delta d_s/\delta t$ (mm/s)	σ_n (MPa)
MB-DS-35	100.70	89.50	9012.65	0.0001	0.5
MB-DS-33	100.40	88.60	8895.44		1.0
MB-DS-30	100.70	89.62	9024.73		1.5
MB-DS-31	100.70	90.20	9083.14		2.0
MB-DS-38	100.80	89.40	9011.52	0.001	0.5
MB-DS-23	100.00	90.00	9000.00		1.0
MB-DS-24	100.70	89.10	8972.37		1.5
MB-DS-37	101.00	89.40	9029.40		2.0
MB-DS-16	100.40	92.60	9297.04	0.01	0.5
MB-DS-08	100.60	88.90	8943.34		1.0
MB-DS-19	100.70	88.00	8861.60		1.5
MB-DS-12	100.88	87.00	8776.56		2.0
MB-DS-15	101.00	89.10	8999.10	0.1	0.5
MB-DS-14	100.56	89.20	8969.95		1.0
MB-DS-17	100.70	89.82	9044.87		1.5
MB-DS-20	103.00	89.72	9241.16		2.0

Table 3.2 The sample dimensions for constant normal stiffness test.

Sample No.	Length (mm)	Width (mm)	Shear area (mm^2)	$\delta d_s/\delta t$ (mm/s)	σ_n (MPa)
MB-DS-39	101.90	87.70	8936.63	0.0001	0.5
MB-DS-40	101.90	87.70	8936.63		1.0
MB-DS-41	102.20	92.50	9453.50		1.5
MB-DS-42	101.60	91.40	9286.24		2.0
MB-DS-43	102.68	92.86	9534.86	0.001	0.5
MB-DS-44	102.14	87.96	8984.23		1.0
MB-DS-45	101.98	85.12	8680.54		1.5
MB-DS-46	104.54	89.84	9391.87		2.0
MB-DS-47	101.98	82.12	8374.60	0.01	0.5
MB-DS-48	101.74	81.00	8240.94		1.0
MB-DS-49	104.24	83.32	8685.28		1.5
MB-DS-50	104.30	84.44	8807.09		2.0
MB-DS-51	101.94	85.96	8762.76	0.1	0.5
MB-DS-52	101.00	86.64	8750.64		1.0
MB-DS-53	102.32	87.22	8924.35		1.5
MB-DS-54	100.98	86.12	8696.40		2.0

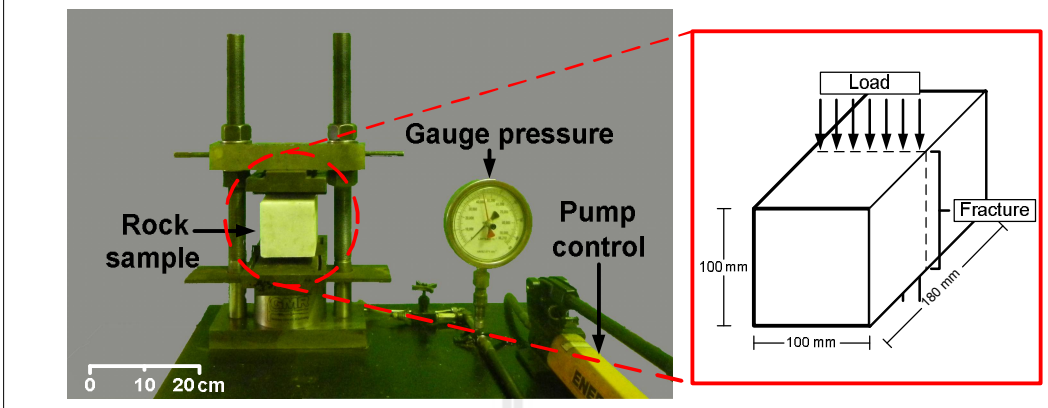

Figure 3.2 100×100×180cubic millimeters block of rock specimen is line-loaded technique by tension inducedmethod.

CHAPTER IV

LABORATORY TESTING

4.1 Introduction

The objective of the laboratory testing is to assess the effects of shear displacement rate on fracture shear strengths by performing series of direct shear testing on tension-induced fractures in saraburi marble specimens. The testing is conducted under CNL and CNStest conditions. The changes of the displacement, initial normal stress and the applied shear stress are monitored. This chapter describes the test apparatus and initial result under CNL and CNS test conditions.

4.2 Test apparatus

A true triaxial load frame is used to apply moved and shear stresses to the specimens (Figure 4.1).The true triaxial load frame has mutually perpendicular 3 pair of steel plates. Four pillars secure each pair.Each pair has spacing about 61 cm^2. The steel plates have dimension of 43×43×4 cm^3 and other twoare 30×30×6 cm^2. Six hydraulic load cells have capacity of 10,000 psi. Diameter of hydraulicload cell is 9 cm^2. One of the lateral stresses(horizontal) is set perpendicular to the fractures plane, which is designated as normal stress (σ_n).The shear stress (τ) is applied by top hydraulic load cell.The bottom hydraulic pump is fixed.Two dial gagesare used for monitoring the normal and shear displacement. The hydraulic pump control normal load is applied to rock specimens for CNL test conditionsas shown in Figure 4.2.The load cell connected with linear volte displacement

transformer (LVDT) are installed and recorded for CNS test conditions as shown in Figure 4.3.

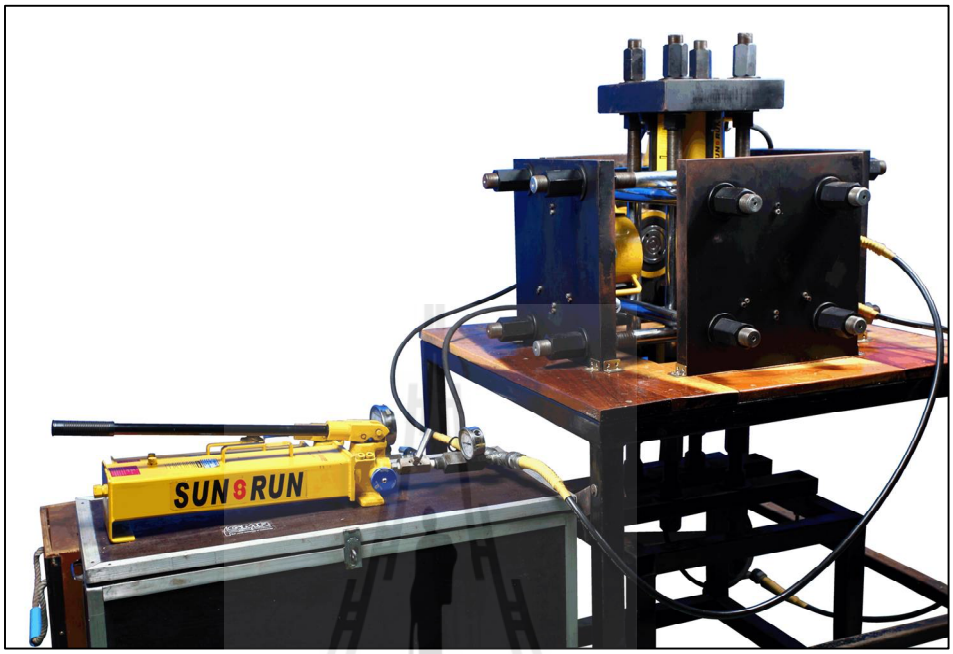

(a) True triaxial load frame

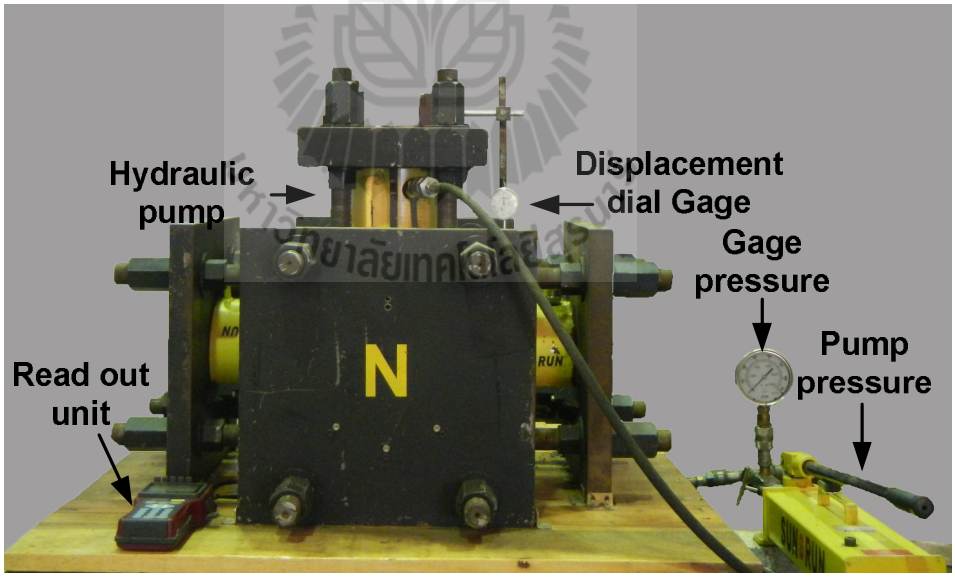

(b) Direct shear test set up

Figure 4.1 True triaxial load frame used in this study.

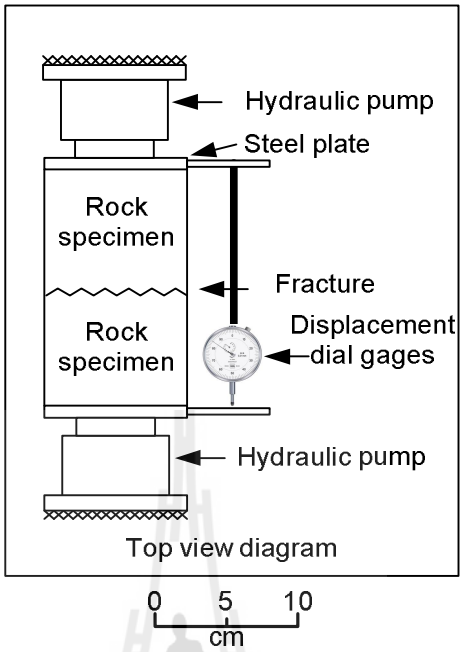

Figure 4.2 Pump and dial gages installed for CNL test condition.

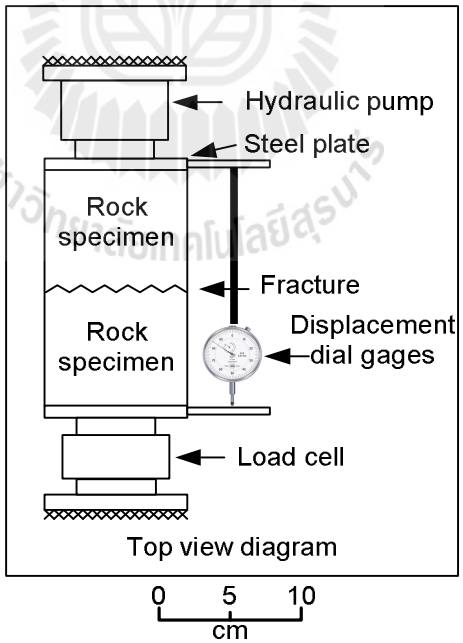

Figure 4.3 Load cell and dial gages installed for CNS test condition.

4.3 Test procedure

The CNL and CNS test conditions are performed with the initial normal stresses of 0.5, 1.0, 1.5 and 2.0 MPa for the rough fractures. Each specimen is sheared only once under the predefined constant normal load or constant normal stiffness. The laboratory arrangement of the direct shear test is performed by that the fracture is under normal and shear stresses for CNL test conditions as shown in Figure 4.4 and Figure 4.5 for CNL test conditions. The shearing displacement rates are 10^{-4}, 10^{-3}, 10^{-2} and 10^{-1} mm/s. The shear force is continuously applied until a total shear displacement of 10 mm is reached. The applied normal and shear forces and the corresponding normal and shear displacements are monitored and recorded.

The CNL test conditions control normal load is constant by hydraulic pumps applied to rock specimen various 0.5, 1.0, 1.5 and 2.0 MPa and shearing vary 10^{-4}, 10^{-3}, 10^{-2} and 10^{-1} mm/s. The normal displacement and shear stresses are record by human.

The CNS test conditions are installed load cell with linear volte displacement transformer (LVDT) for normal load recorded and gage pump pressure installed for shear stresses recorded. The test results are record by human.

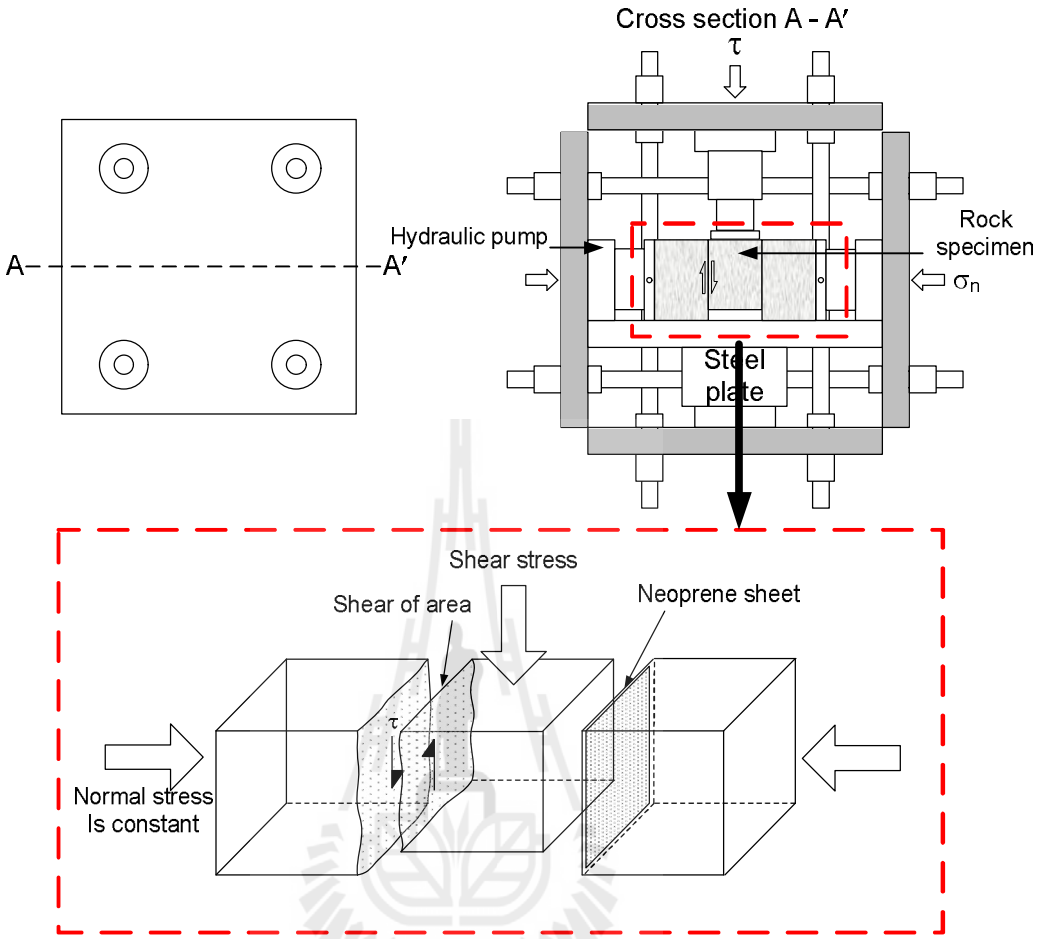

Figure 4.4 The laboratory arrangementsfor CNL test conditions.

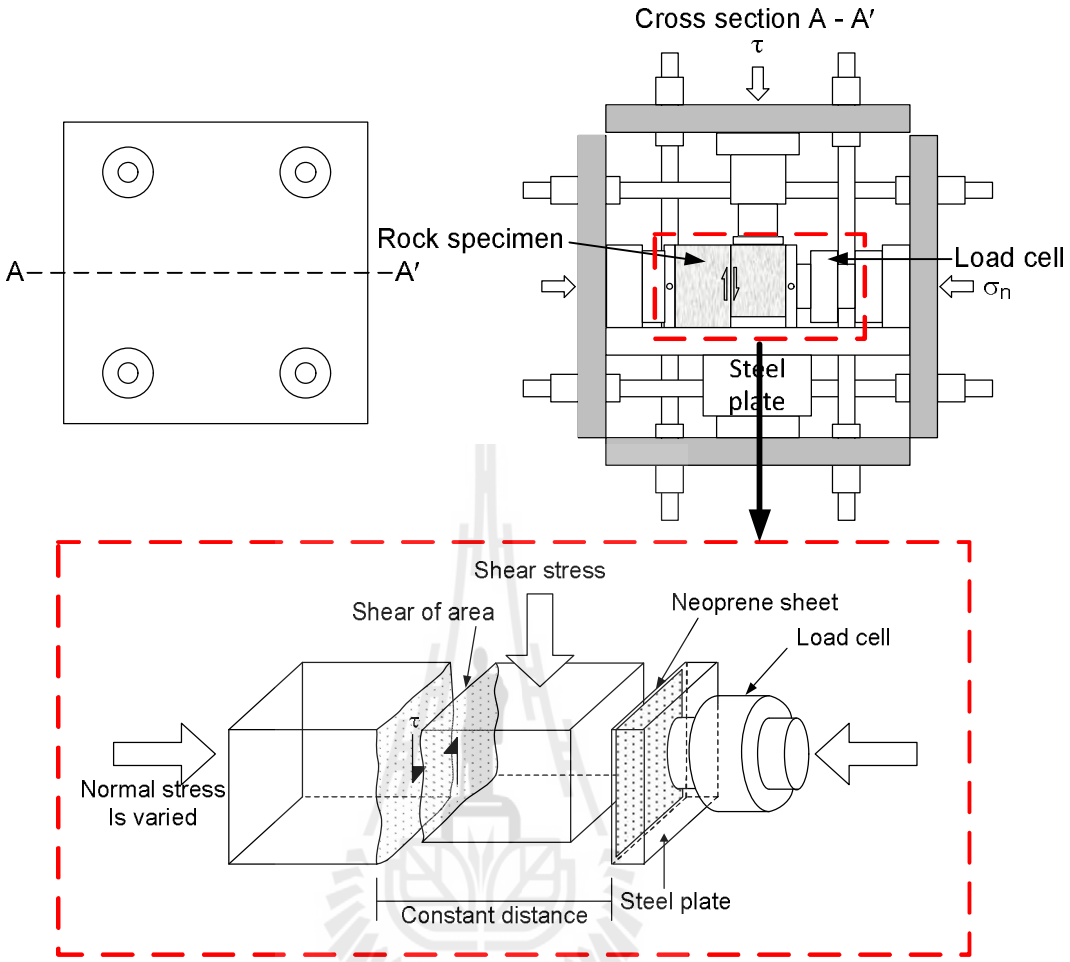

Figure 4.5 The laboratory arrangements for CNS test conditions.

CHAPTER V

TEST RESUTLS

5.1 Introduction

This chapter describes the test results of direct shear tests on tension-induced fractures in Saraburi marble under the CNL and CNS test conditions. They are presented in terms of the shear stresses as a function of shear displacement. The shear strengths are presented as a function of normal stresses. The effects of shear rate are also discussed.

5.2 CNL test conditions

The shear strengths test are determined for shear displacement rates ranging from 10^{-4} to 10^{-1} mm/s with the constant normal stresses from 0.5, 1.0, 1.5 to 2.0 MPa for CNL test conditions. The results are presented in forms of shear stress-shear displacement curves, shear-normal stresses, fracture dilations and post-test observations.

5.2.1 Shear stress- displacement curves

The shear stress-displacement (τ-d_s) curves shows peak shear stresses as a function of shear displacement under various normal stresses and shear displacement rates for the CNL test conditions in Figure 5.1. It is clear that the shear strengths increase with increasing the normal stresses and shear displacement rates. The effects of shear stresses tend to be enhanced under high normal stress and high shear displacement rates.

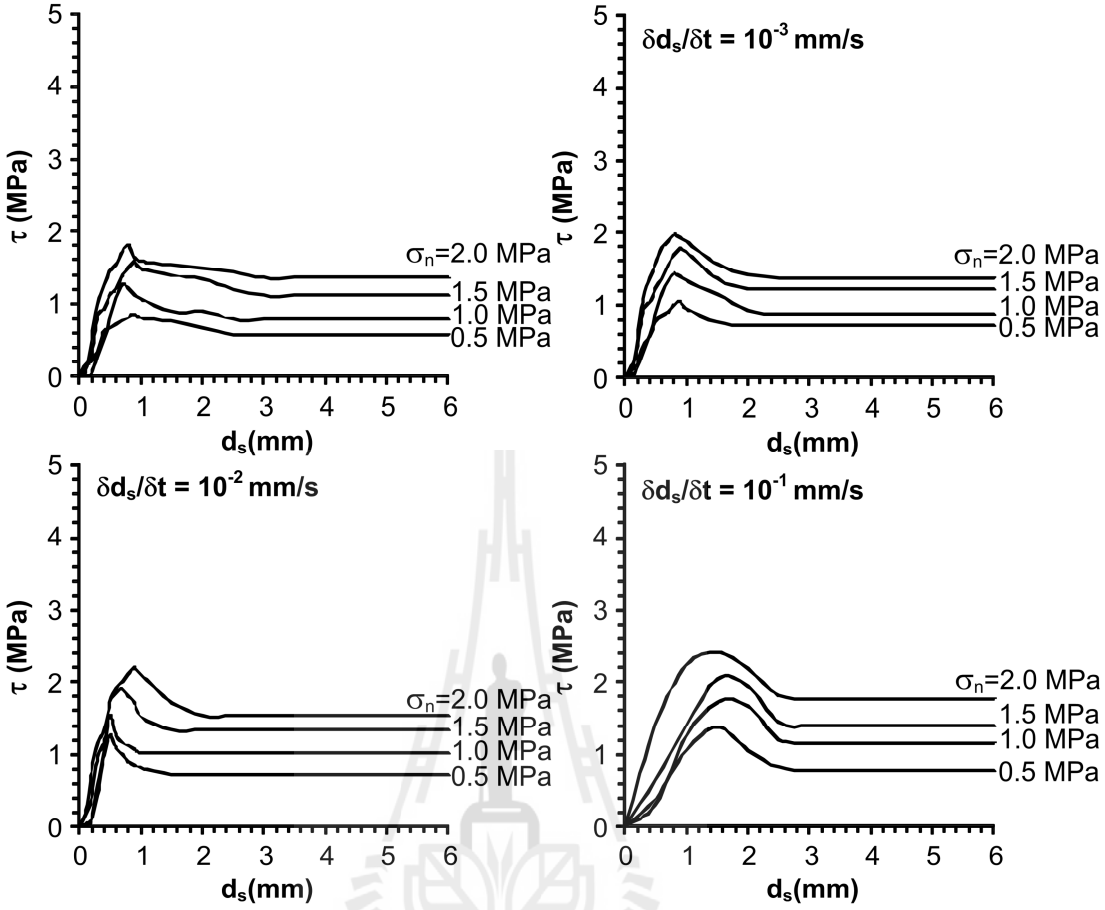

Figures 5.1 Peak shear stresses (τ_p) as a function of shear displacement (d_s) for various displacement rates ($\delta d_s/\delta t$) of CNL test conditions.

5.2.2 Shear-normal stresses diagrams

Table 5.1 summaries the results of peak shear strength for CNL test conditions. Figure 5.2 plots the peak shear stresses as a function of normal stresses under various shear displacement rates ($\delta d_s/\delta t$). The peak shear stresses increases shear displacement rates. Linear behavior of the τ_p-σ_n relation is observed. Again the effects of the shear displacement rates can be seen by the reduction of the peak shear stresses as the shear displacement rates decrease.

Table 5.1 Summary of peak shear stresses for all shear displacement rates under CNL test conditions.

$\delta d_s/\delta t$ (mm/s)	τ_p (MPa)			
	σ_n=0.5	1.0	1.5	2.0
0.0001	0.861	1.267	1.580	1.819
0.001	1.048	1.431	1.781	1.975
0.01	1.267	1.538	1.909	2.251
0.1	1.377	1.718	2.039	2.408

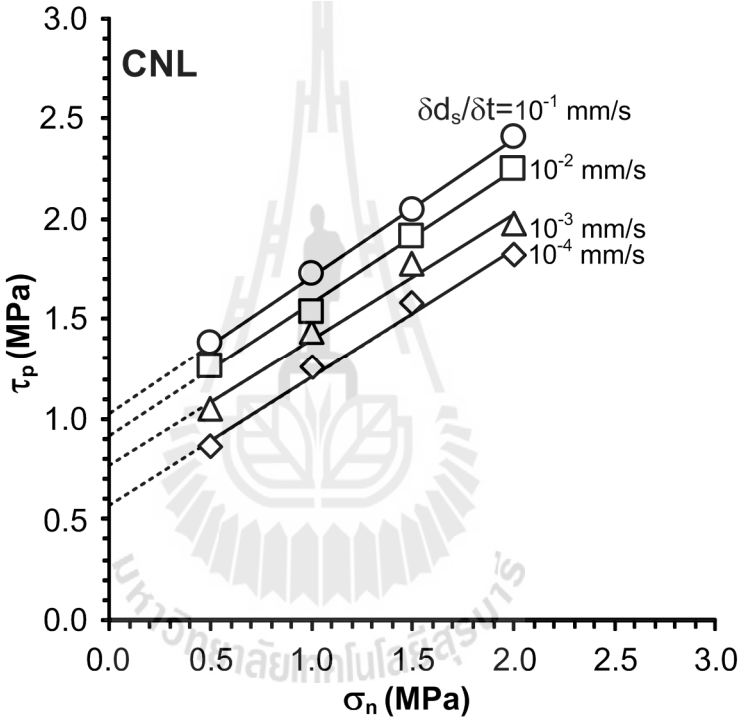

Figure 5.2 Peak shear stresses as a function of normal stresses for CNL test conditions.

5.2.3 Fracture dilation

Dilation is the normal separation of the fractures walls, induced by the shearing movement of the fracture. The amount of dilation is governed by the fracture roughness, joint wall strength and the applied normal stresses. Here an assessment of the shear displacement rates effect on the fracture dilation has been made. Figure 5.3 shows the normal displacement as a function of shear displacement for various shear

displacement rates obtained from the CNL test conditions. The effects of the normal stress and shear displacement rates can be revealed from the d_n-d_s diagrams. The dilations increase with increasing shear displacement, shear displacement rates.

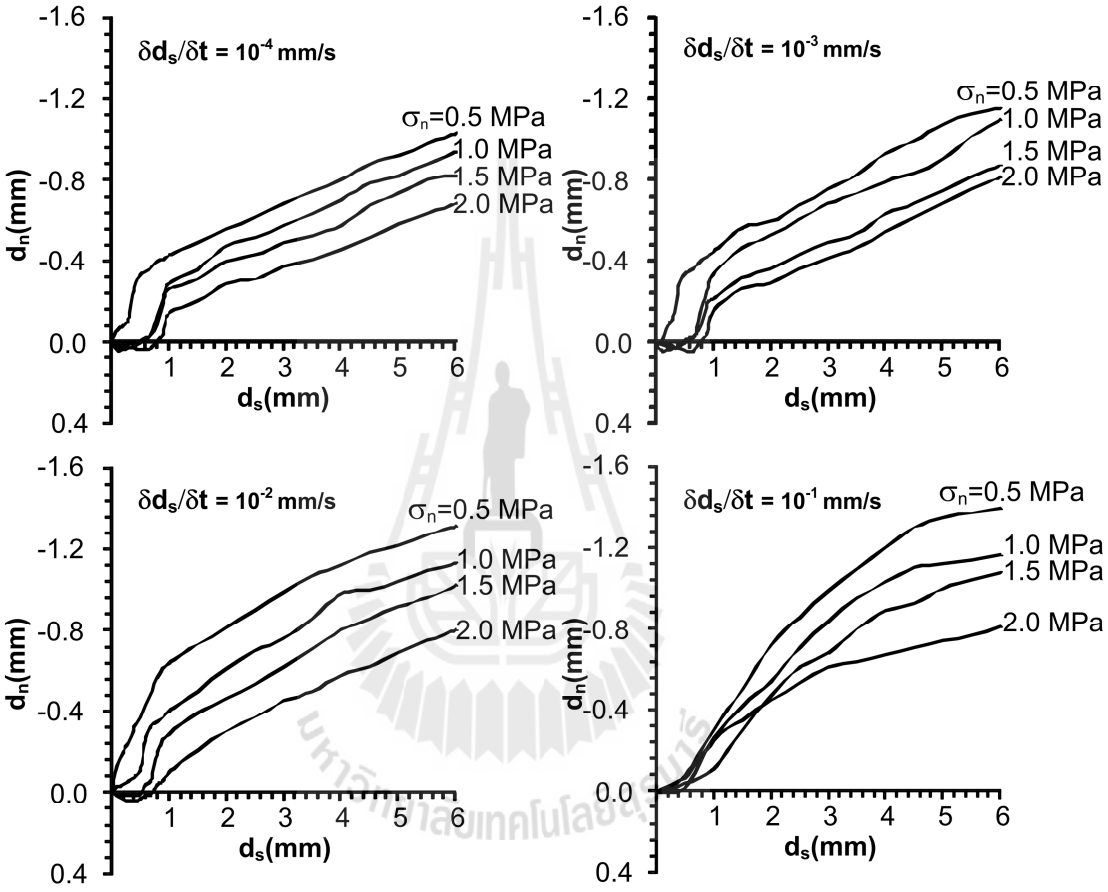

Figures 5.3 Normal displacements as a function of shear displacement for various shear displacement rates obtained from CNL test conditions.

5.2.4 Post-test observations

Post-test fractures have been examined in attempt to qualitatively correlate the sheared-off areas with the normal stresses and shear displacement rates. A difficulty arises for this task. The post-test fractures are observed by the deposition of the rock powder resulting from the crushing of the asperities. Nevertheless, some conclusions can be drawn. As expected, the increase of the normal stresses significantly increases the sheared-off areas for CNL test conditions. The reduction of the shear displacement rates also increases the sheared-off areas. These agree reasonably well with the fracture dilation measured during the test that both normal stresses and reduction of the shear displacement rates can clearly minimize the amount of dilation which results in an increase of the amount of the sheared asperities.

5.3 CNS test conditions

The constant normal stiffness tests are performed under shear displacement rates ranging from 10^{-4} to 10^{-1} mm/s with the initial normal stresses from 0.5, 1.0, 1.5 to 2.0 MPa. The results are presented in forms of shear stress-shear displacement curves, Normal displacement-normal stresses diagrams, fracture dilations and post-test observations. The shear strengths as a function of normal stresses shear displacement rate and shear displacement of the fractures during shearing.

5.3.1 Shear stress-shear displacement curves

Table 5.2 shows the results for CNS test conditions. The shear stress-displacement (τ-d_s) curves are shown in Figures 5.4. The shear strengths increase with increasing the initial normal stresses and shear displacement rates. The effects of shear stresses tend to be enhanced under high normal stress and high shear displacement rates.

Table 5.2 Summary of peak shear stresses for all shear displacement rates under CNS test conditions.

$\delta d_s/\delta t$ (mm/s)	τ_p (MPa)			
	σ_n=0.5	1.0	1.5	2.0
0.0001	2.550	3.182	3.837	4.733
0.001	2.958	3.980	4.570	5.413
0.01	4.128	4.980	5.857	6.680
0.1	5.038	5.532	6.647	7.370

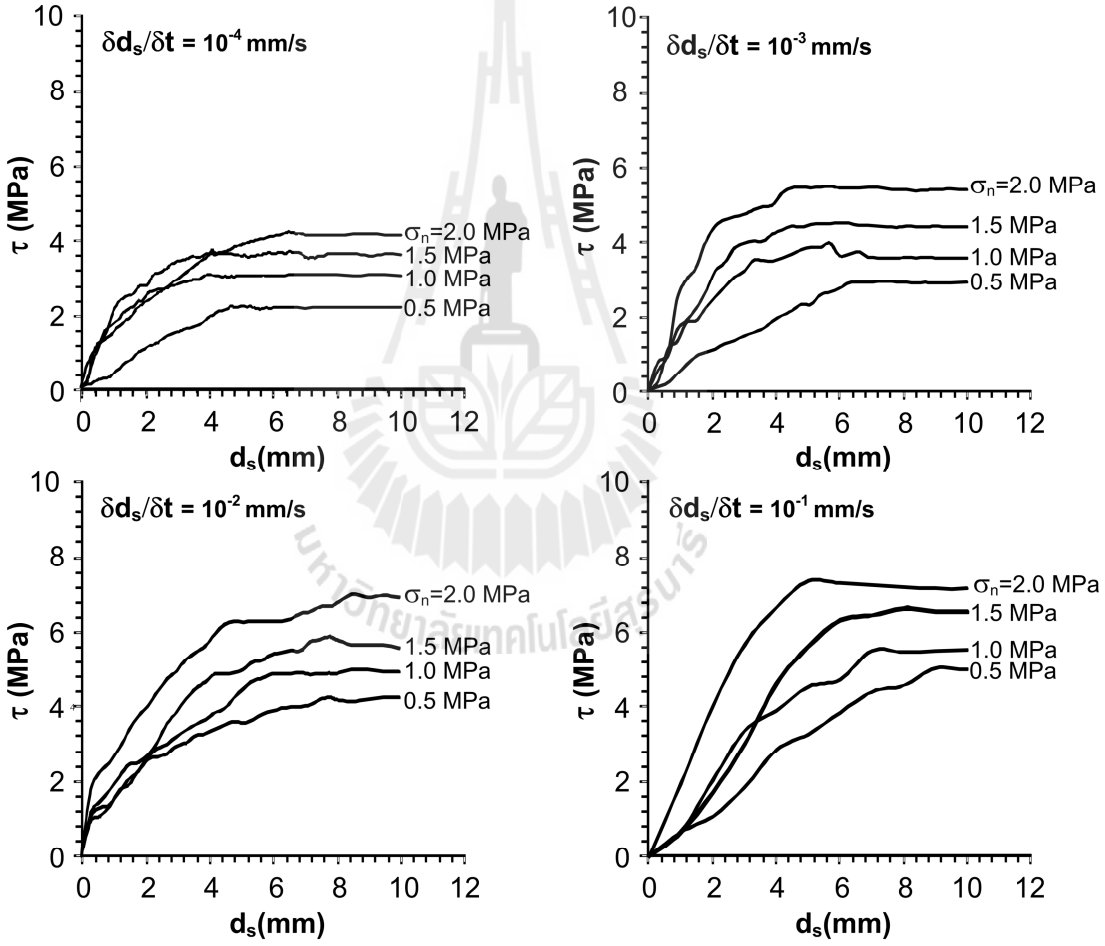

Figures 5.4 Peak shear stresses (τ_p) as a function of shear displacement (d_s) for various displacement rates ($\delta d_s/\delta t$) of CNS test conditions.

5.3.2 Shear stresses - normal stresses

Figures 5.5 plots the peak shear stresses as a function of normal stresses under various shear displacement rates ($\delta d_s/\delta t$) for the CNS test conditions. The peak shear stresses increase with normal stresses and shear displacement rates. The effects of the shear displacement rates can be seen by the increase of the normal stresses as the shear displacement rates increase.

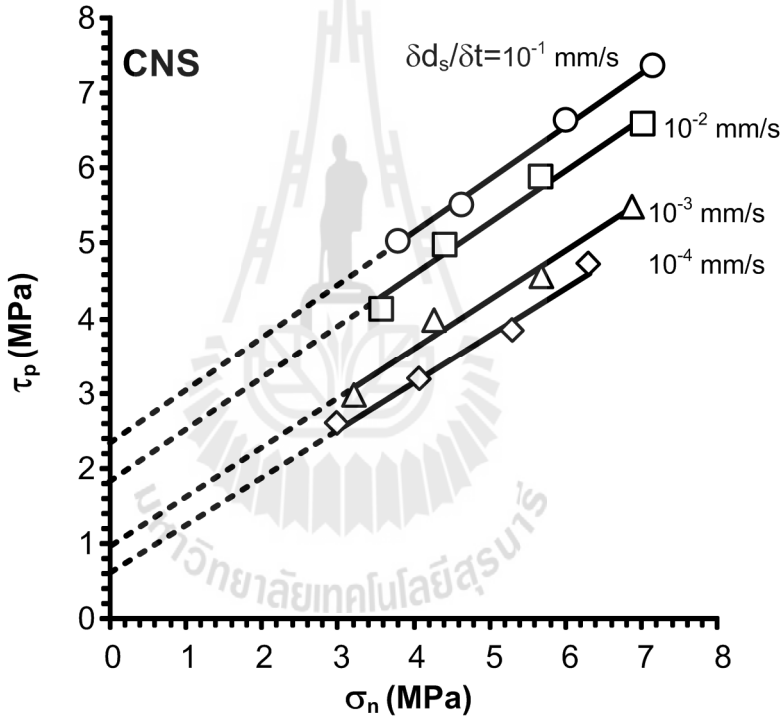

Figure 5.5 Peak shear stresses as a function of normal stresses for CNS test conditions.

5.4 Comparisons between CNL and CNS test conditions

The friction angle (ϕ) and cohesions (c) of the marble fractures under CNL and CNS test conditions are shown in Table 5.3. The CNS has friction angle and cohesion higher than those of the CNL test conditions as shown in Figures 5.6 and 5.7. This suggests that when the fractures are confined or are not effect to dilate (CNS condition) they will have higher shears resistance than tend of unconfined fractures (CNL condition). Post-test observations of the sheared fractures suggest that the higher normal stresses and shear displacement rates are applied, that larger sheared of areas are obtained, as shown in Figures 5.8 through 5.11 under CNL and CNS test conditions.

Table 5.3 Summary of frictions angles and cohesions for all shear displacement rates under CNL and CNS test conditions.

$\delta d_s/\delta t$(mm/s)	CNL		CNS	
	$\tau = \sigma_n \tan\phi + c$		$\tau = \sigma_n \tan\phi + c$	
	ϕ (Degree)	c (MPa)	ϕ (Degree)	c (MPa)
0.0001	32.21	0.585	32.59	0.601
0.001	32.05	0.776	33.63	0.923
0.01	33.61	0.911	35.08	1.754
0.1	34.32	1.032	35.64	2.289

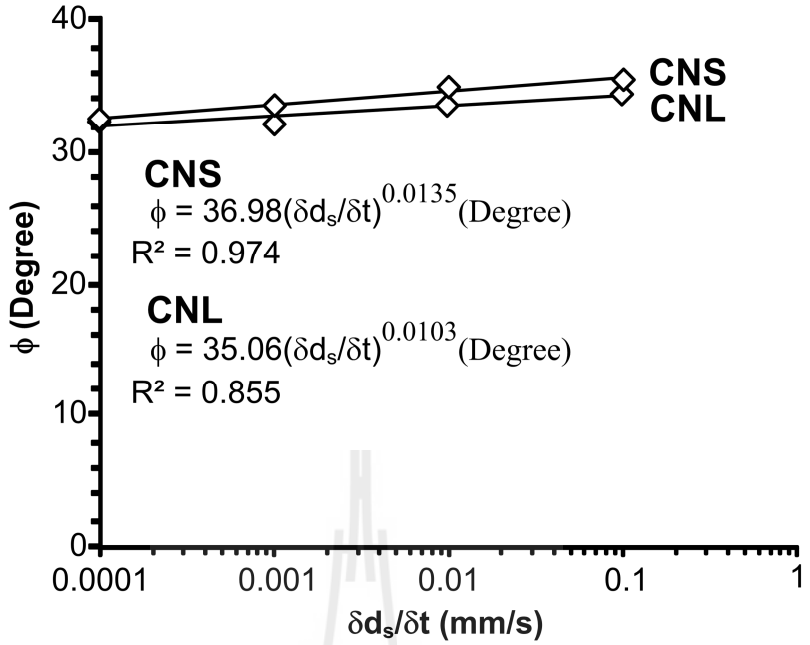

Figure 5.6 Friction angle as a function of shear displacement rates ($\delta d_s/\delta t$) under CNL and CNS test conditions.

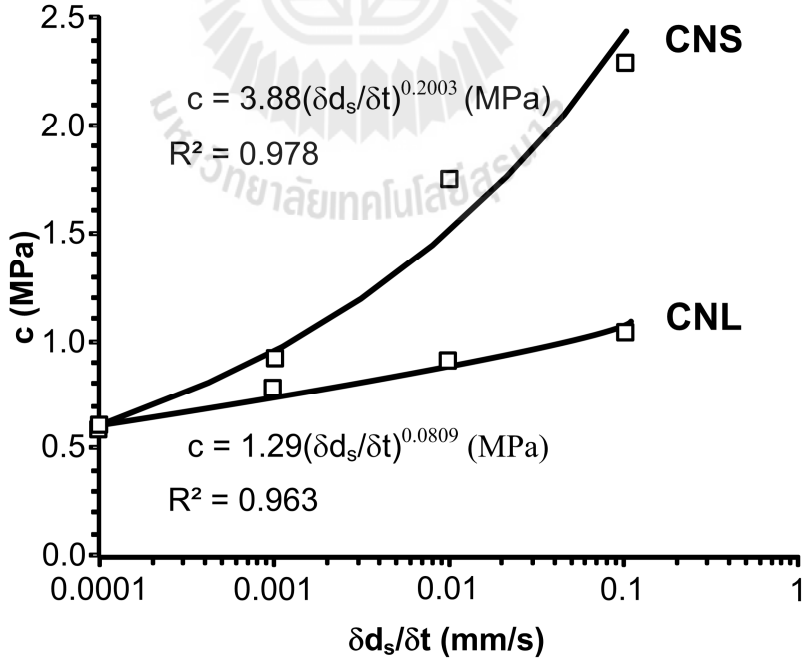

Figure 5.7 Cohesions as a function of shear displacement rates ($\delta d_s/\delta t$) under CNL and CNS test conditions.

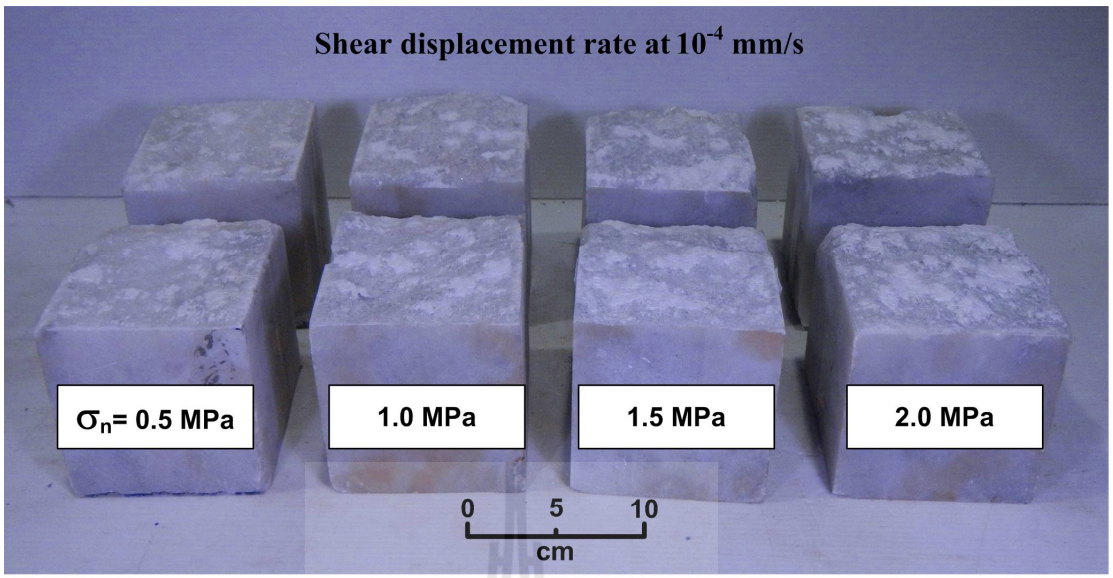

(a)

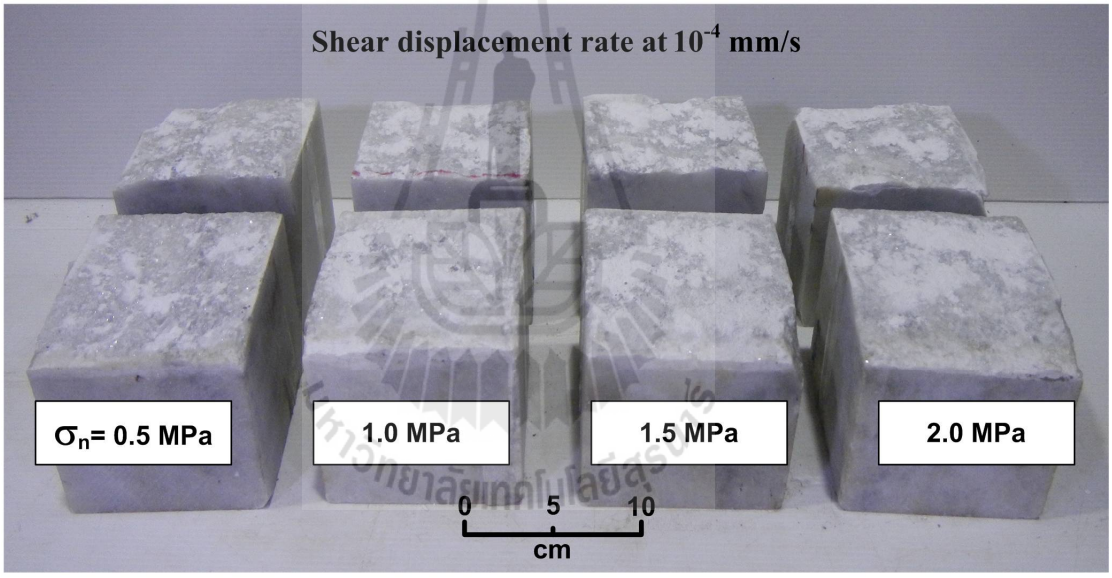

(b)

Figures 5.8 Post-test specimens from direct shear test under initial normal load and shear displacement at 10^{-4} mm/s under CNL (a) and CNS test conditions (b).

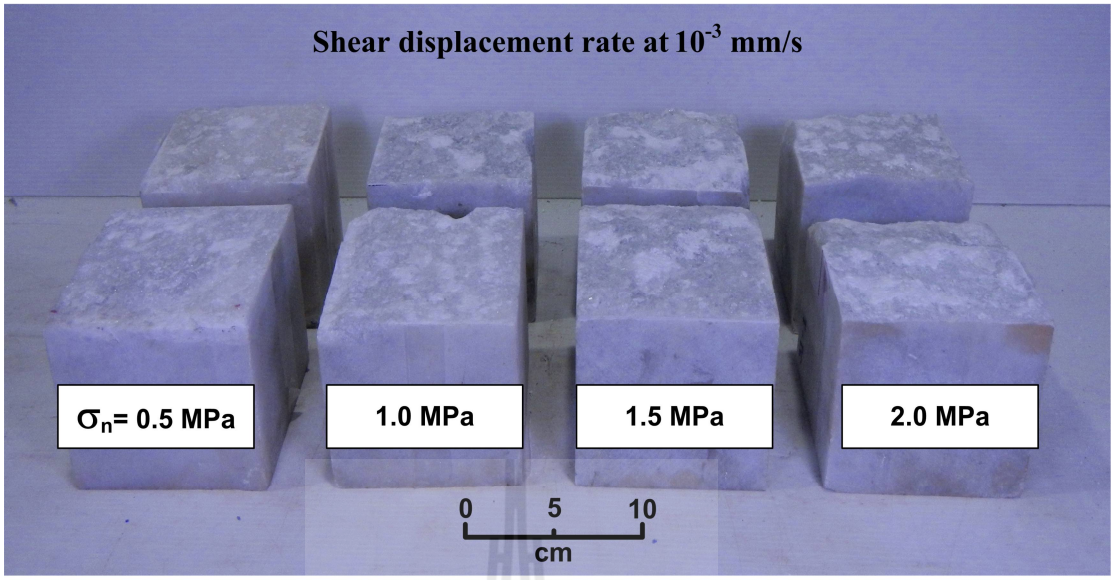

(a)

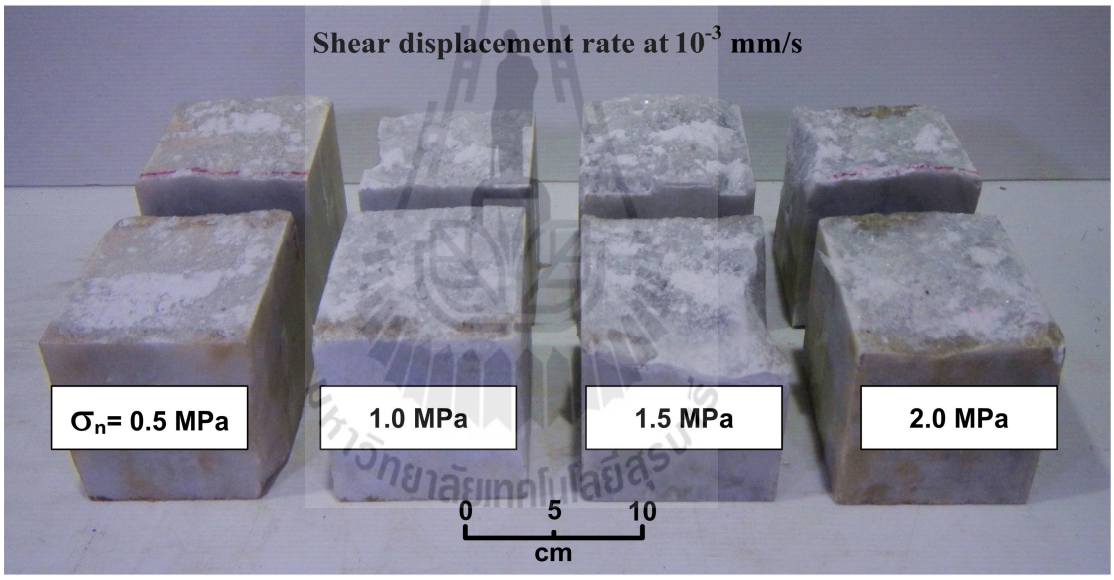

(b)

Figures 5.9 Post-test specimens from direct shear test under initial normal load and shear displacement at 10^{-3} mm/s under CNL (a) and CNS test conditions (b).

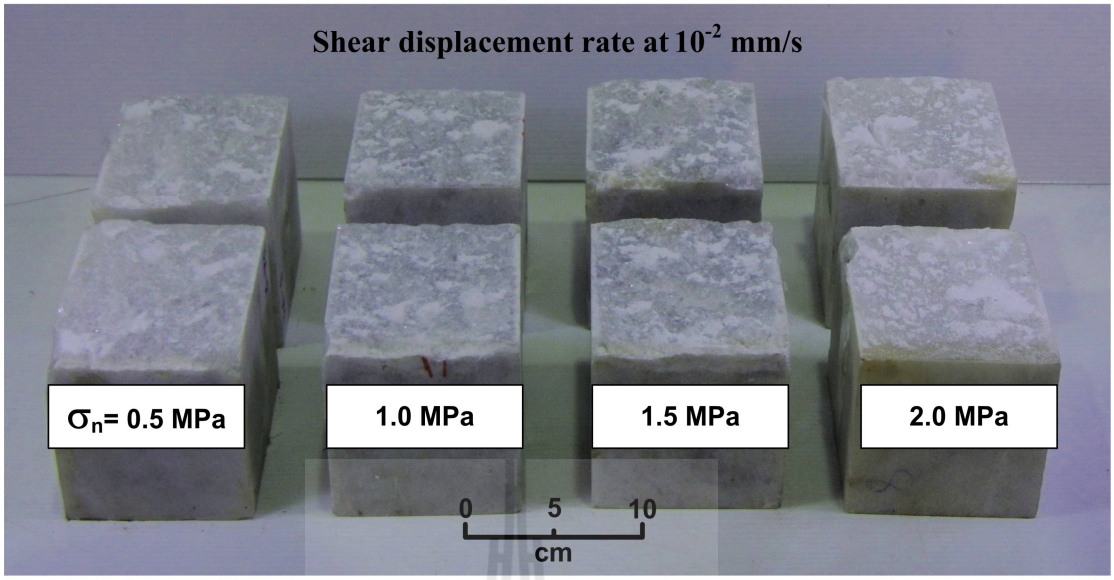

(a)

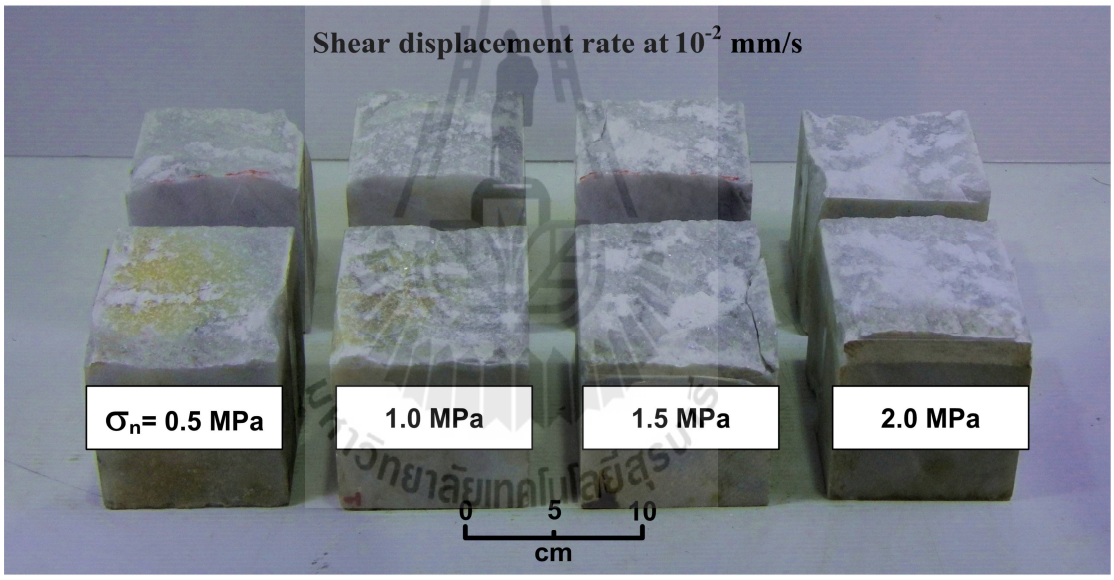

(b)

Figures 5.10 Post-test specimens from direct shear test under initial normal load and shear displacement at 10^{-2} mm/s under CNL (a) and CNS test conditions (b).

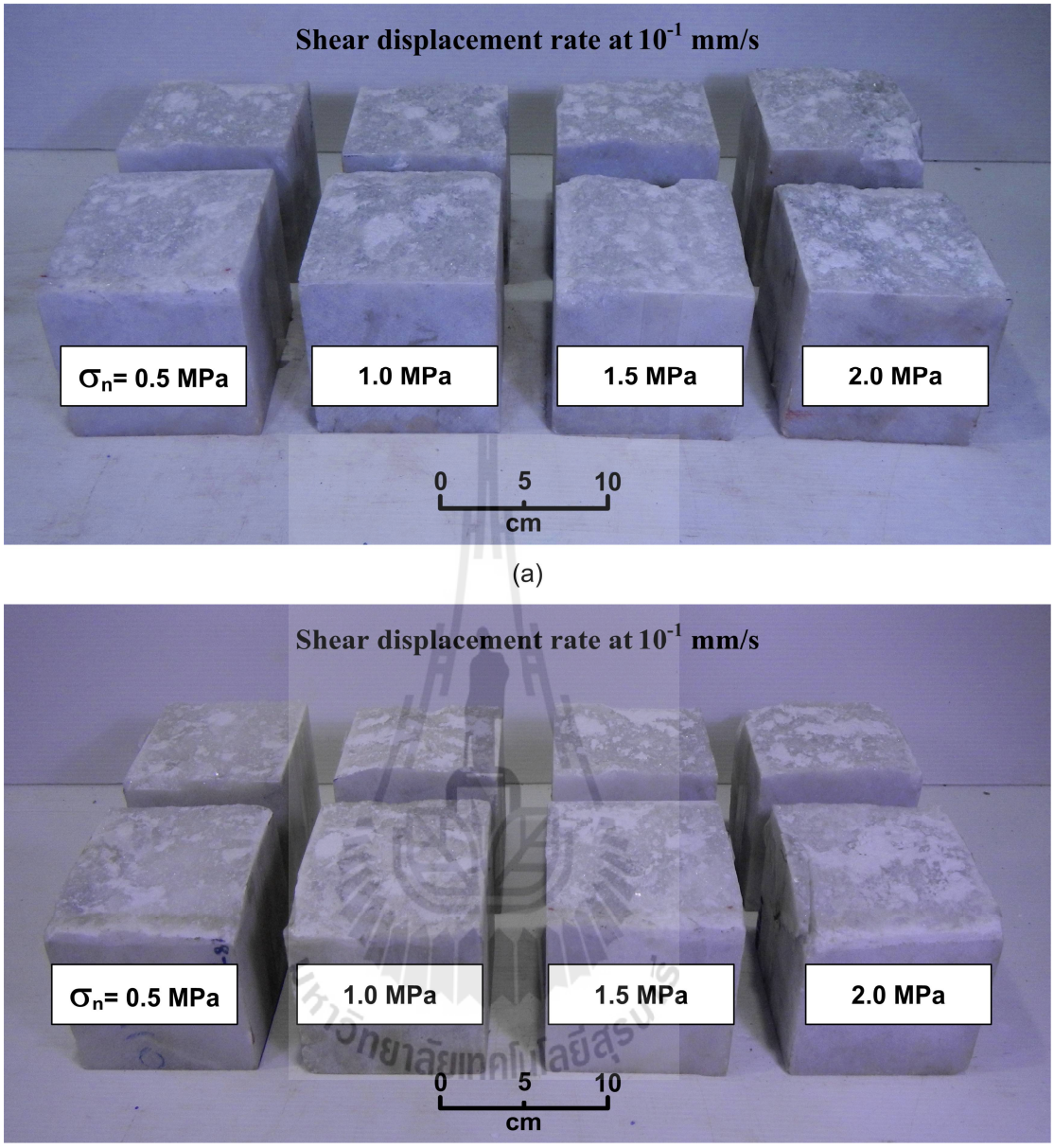

Figure 5.11 Post-test specimens from direct shear test under initial normal load and shear displacement at 10^{-1} mm/s under CNL (a) and CNS test conditions (b).

CHAPTER VI

ANALYSIS

6.1 Introduction

The objective of this chapter is to describe the analysis shear strength and to experimentally determine the shear strength of jointed rock specimen under true triaxial load frame. The effort involves performing direct shear tests on specimen which vary normal stresses and displacement rates. The shear strengths are analyzed by Coulomb criteria, effect of normal stresses and effect of displacement rates. The results are compared between CNL and CNS test conditions.

6.2 Analysis by Coulomb criteria

Based on the Coulomb criterion, the shear stress (τ) can be represented by:

$$\tau = c + \sigma_n \tan \phi \qquad \text{(MPa)} \qquad (6.1)$$

where σ_n is the normal stress, c is the cohesion and ϕ is the friction angle. The cohesion and friction angle of all specimens of CNL and CNS test conditions are summarized in Table 5.3. They can be determined as a function of the shear displacement as follows (Figures 6.1):

$$c = \beta \, (\delta d_s/\delta t)^{\chi} \qquad \text{(MPa)} \qquad (6.2)$$

$$\phi = \kappa (d_s/\delta t)^{\lambda} \qquad \text{(Degree)} \qquad (6.3)$$

where parameters β, χ, κ and λ are empirical constants as shown in Table 6.1. Substituting equations (6.2) and (6.3) into (6.1), the shear strength (τ) can be written as:

$$\tau = [\ \beta(\delta d_s/\delta t)^{\chi}\ ] + \sigma_n \tan [\ \kappa(\delta d_s/\delta t)^{\lambda}\ ] \text{ (MPa)} \quad (6.4)$$

The compared peak shear strength under various shear displacement rates of CNL and CNS test conditions based on Coulomb derived equation and result tested. The result is fit similar. The CNL and CNS test conditions are plots peak shear strength as a functions of normal stresses and various displacement rates as shown in Figures 6.2.

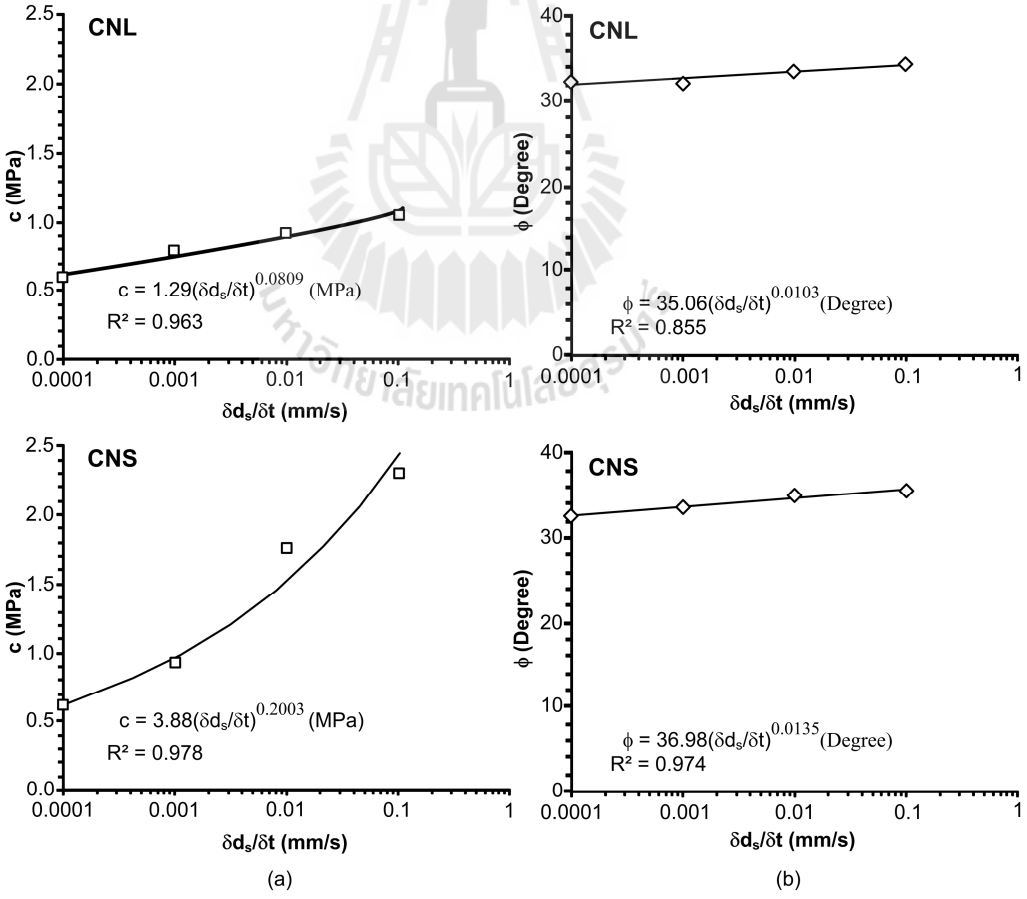

Figures 6.1 Cohesions (c) and frictions angle (ϕ) as function of shear displacement rates under CNL (a) and CNS test conditions (b).

Table 6.1 Constants β, χ, κ and λfor all tested conditions.

Tested conditions	β	χ	κ	λ
CNL	1.29	0.0809	35.06	0.0103
CNS	3.88	0.2003	36.98	0.0135

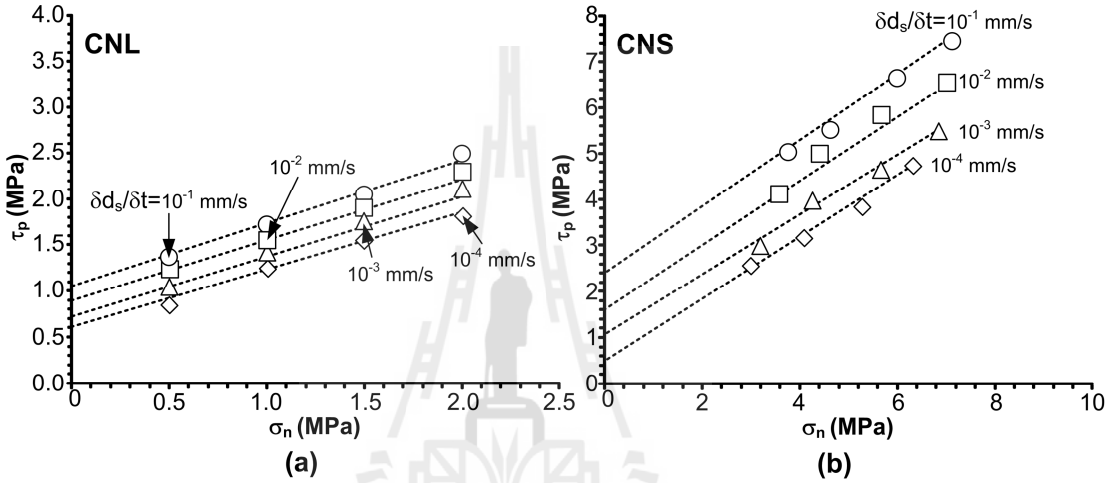

Figures 6.2 Peak shear strength under various shear displacement rates of CNL (a) and CNS test conditions (b) on derived equation (dash line) and results tested (symbol).

6.3 Effect of normal stresses

The CNL test conditions control normal stresses are constant. The applied initial normal stresses to CNS test conditions. The normal stresses effect to peak shear strengths are increases under CNL and CNS test conditions. The results of CNS test conditions have peak shear strength higher than CNL test conditions (Figure 6.2).

6.4 Effect of displacement rates

The CNL and CNS test conditions are tested with displacement rates from 10^{-4} to 10^{-1} mm/s. The shear displacement rate effect to peak shear strengths increases under CNL and CNS test conditions. The shear strengths increase with increasing the shear displacement rates under CNL (Figure 5.1) and CNS test conditions (Figure 5.4). The normal stresses increase with increasing the shear displacement under CNS test conditions (Figure 6.3). The results of CNS test conditions show peak shear strength higher than CNL test conditions (Figure 6.2) when plotted as a function of shear displacement rates.

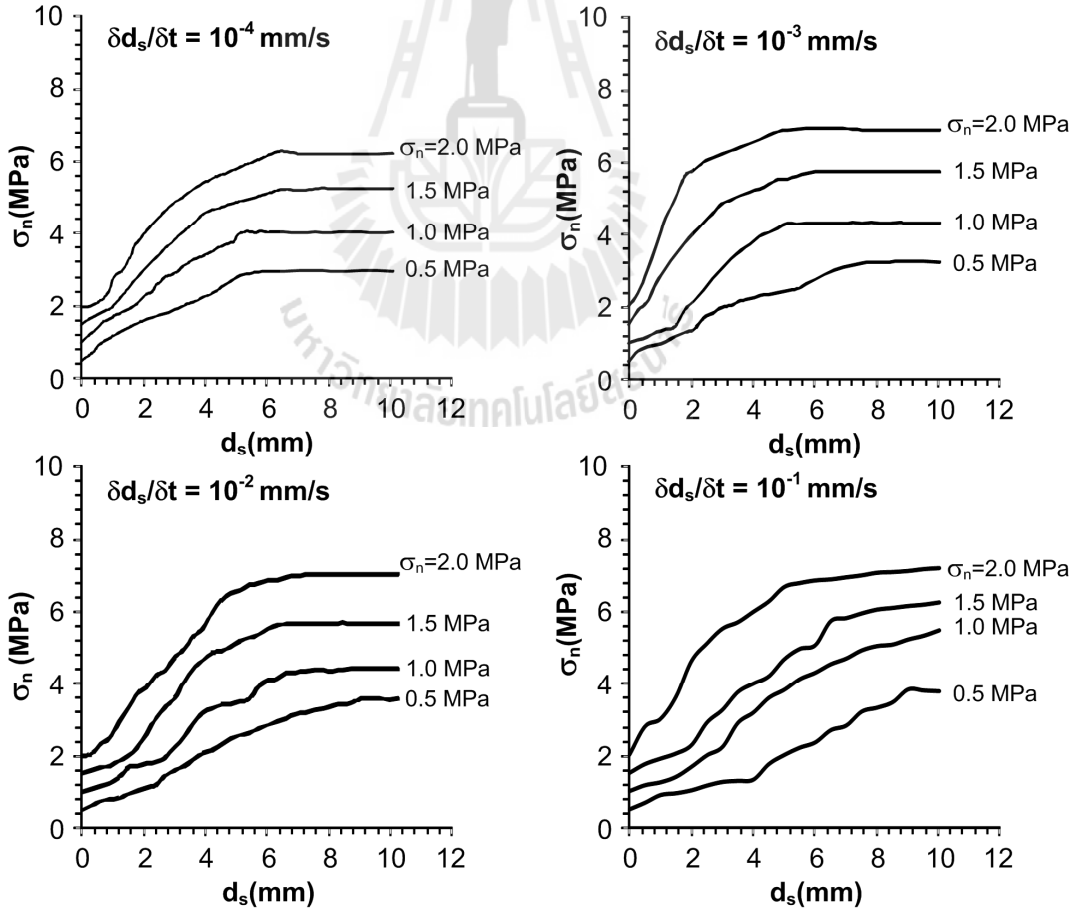

Figures 6.3 Normal stresses as a function shear displacement various initial normal stresses under CNS test conditions.

CHAPTER VII

DISCUSSIONS, CONCLUSIONS AND RECOMMENDATIONS FOR FUTURE STUDIES

7.1 Discussions

The shear displacement rates can affect the shear strengths of the tension-induced fractures in the Saraburi marble. Here the Coulomb's criterion can well describe the joint shear strengths of the rocks under the shear displacement rates ranging from 10^{-4} to 10^{-1} mm/s with the normal stresses from 0.5 to 2 MPa for CNL and CNS test conditions. The higher the peak shear strengths are obtained particularly under high normal stresses and high shear displacement rates. As a result the cohesion and friction angle obtained for the Coulomb criterion can be correlated among different shear displacement rates. It is found that both cohesion and friction angle notably increase with the shear displacement rates. The CNS test condition gives higher cohesions and friction angle than CNL test conditions. The cohesion is about 0.585 MPa under the shear displacement rate of 10^{-4} mm/s to about 1.032 MPa under the shear displacement rate of 10^{-1} mm/s for CNL conditions. The cohesion is about 0.601 MPa under the shear displacement rate of 10^{-4} mm/s to about 2.289 MPa under the shear displacement rate of 10^{-1} mm/s for CNS conditions. The friction angles are about 32.21 degree under the shear displacement rate of 10^{-4} mm/s to about 34.32 degree under the shear displacement rate of 10^{-1} mm/s for CNL conditions. The friction angles are about 32.59 degree under the shear displacement rate of 10^{-4} mm/s

to about 35.64 degree under the shear displacement rate of 10^{-1} mm/s for CNL conditions.

The friction angles slightly increase when the shear displacement rates increase from 10^{-4} to 10^{-1} mm/s under both CNL and CNS test conditions. The slope of normal and shear displacement curve (dilation) are higher for higher displacement rates and the higher normal stress and lower dilation. The scattering of the data is probably due to the intrinsic variability of the tested fractures.

The shear strengths are clearly dependent of the shear velocities. This suggests that the rate-dependent shear strength and stiffness of the tension-induced fractures is primarily due to the time-dependent strength of the rock asperities on the fracture wall. This supported by the experimental results obtained by Fuenkajorn and Khenkhunthod (2010) who conclude that the uniaxial and triaxial compressive strengths and elastic modulus of the three sandstones increase exponentially with the loading rate. It can therefore be postulated that the time-dependent shear strengths of the fractures may be found in other rock types of which compressive strengths are sensitive to loading rate. The comparison of **Tables 6.1** and **6.2** shows the time-dependent shear strength that relates to the rock strength.

Table 7.1 The compressive strength PW of Fuenkajorn and Khenkhunthod (2010).

$\delta\sigma_1/\delta t$ (MPa/s)	Compressive strength, σ_c (MPa)			
	Confining stress = 0 MPa	3 MPa	7 MPa	12 MPa
10	83.50	110	130	145
1.0	68.60	102	121.67	146.62
0.1	64.62	85.50	109.26	143.94
0.01	57.80	80.16	95.48	135.04
0.001	46.80	73.64	90.6	130.20

Table 7.2 The shear strength PW of Fuenkajorn and Khenkhunthod (2010).

$\delta d_s/\delta t$ (mm/s)	Shear strength, τ_{peak} (MPa)			
	Normal stress = 1 MPa	2 MPa	3 MPa	4 MPa
0.1	1.87	2.75	3.27	3.83
0.01	1.69	2.38	2.99	3.55
0.001	1.45	1.91	2.71	3.08
0.0001	1.27	1.82	2.24	2.89

The results of this study agree with the study on time-dependent rock strength by Sang and Dhir (1972) who investigate the influence of strain rate on the strength, deformation and fracture properties of Lower Devonian sandstone. Comparison of strength results obtained at different loading and rates showed that for similar loading times to failure the constant rates of loading give slightly higher strength values. This agrees with the observation by Ray et al. (1999). A clear increase in uniaxial compressive strength is observed with increase in strain rate. Stress is found to increase with the increase in strain rate and Young's modulus was found to increase with the increase in strain rate. However, this study disagrees with the result by Jafari et al. (2003), who study the effects of displacement rates (or shearing velocity) on

shear strength. It is observed that shear strength reduces with increasing shears velocity, approaching the same values for the peak and residual strength at higher shearing velocities. They study on smaller range of shear velocities, while this study has large range of shear velocities.

7.2 Conclusions

The shear displacement rates can affect the shear strengths of the tension-induced fractures in the Saraburi marble for both CNL and CNS test conditions. As a result the cohesion and friction angle obtained for the Coulomb criterion can be correlated among different shear displacement rates. The higher initial normal stresses and higher shear displacement rates are applied the high peak shear strength is obtained. The CNS shows the effect of rock joint more than the CNL test conditions. The comparisons between CNL and CNS test conditions are demonstrated as the effect on peak shear strength (τ_p), cohesion (c), friction angle (ϕ).

This study is aimed to experimentally assess effect of shear displacement rates on joint shear strength and joint stiffness of fracture marble. The results indicate that the initial normal stresses and shear displacement rates are effect on peak shear strength (τ_p), cohesion (c), friction angle (ϕ) under CNL and CNS test conditions. The shear behavior of rock joint under CNS test condition is closer to reality than the CNL test condition for certain field applications, particularly in mining excavations.

7.3 Recommendations for future studies

Recognizing that the numbers of the specimens and the test parameters used here are relatively limited, more testing and measurements are recommended, as follows:

(1) The fracture areas used in this study (100×90 mm^2) are relatively small even though they are well complied with the relevant standard practice and internationally suggested method. Testing on larger fracture areas would provide a more representative of the shear strength results when they are applied to the actual fractures under in-situ condition.

(2) Increasing the number of the specimens would statistically enhance the reliability of the test results and the predictability of the proposed strength criterion.

(3) Performing the direct shear tests on a variety of rock types with different fractures, hardness and strengths would improve our understanding of the shear displacement rates effect on the fracture shear strength. In particular the fractures prepared in time-dependent rock would reveal the time-dependent strengths of the fracture rock wall as affected by the shear displacement rates. The knowledge on how the plastic or time-dependent rock wall fractures respond to the shear velocity would be benefit to understand the fault behavior at great depth.

(4) Performing the direct shear tests on a variety of CNL and CNS test conditions with difference initial normal stresses and shear displacement rates.

REFERENCES

ASTM D5607-08. Standard test method for performing laboratory direct shear strength tests of rock specimens under constant normal force. **Annual Book of ASTM Standards**, Vol. 04.08.West Conshohocken, PA: American Society for Testing and Materials.

Babanouri, N., Nasab, S.K., Baghbanan, A., Mohamadi, H.R. (2011). Over-consolidation effect on shear behavior of rock joints. **International Journal of Rock Mechanics & Mining Sciences** 48 (8): 1283-1291.

Bahaaddini M., Sharrock G., B.K. Hebblewhite. (2013). Numerical direct shear test to model the shear behavior of rock joints. **Computers and Geotechnics**. 51 (1):101-115.

Barton N. (2012). Shear strength criteria for rock, rock joints, rockfill and rock masses: Problems and some solutions. **Journal of Rock Mechanics and Geotechnical Engineering** 5: 249–261.

Barton N. R. (1997). The shear strength of rocks and rock joints. **International Journal of Rock Mechanics & Mining Sciences** 34: 255-279.

Brady, B.H.G., Brown, E.T., 2006. Rock Mechanics for Underground Mining (3rd. Edn.). Springer, Netherlands, 628 p.

Fuenkajorn, K., Kenkhunthod, N. (2010). Influence of Loading Rate on Deformability and Compressive Strength of Three Thai Sandstones. **Geotechnical and Geological Engineering**. 28: 707-715.

Grasselli, G., Egger, P. (2003). Constitutive law for the shear strength of rock joints based on three-dimensional surface parameters. **International Journal of Rock Mechanics & Mining Sciences** 40 (1): 25-40.

Hong-rae Rim, Hae-jun Choi, Bong-Ki Son, Chung-In Lee & Jae-Joon Song. (2005). Experimental study for shear behavior of pseudo rock joint under constant normal stiffness condition. **Analysis of the Past and Lessons for the Future – Erdem & Solak (eds)**. ISBN 04 1537 452 9.

Indraratna B., . haque A. (2000). Experiment study of shear behavior of rock joints under constant normal stiffness conditions. . **International Journal of Rock Mechanics & Mining Sciences.** 34 (3-4): 141.e1-141.e15.

Indraratna B., . haque A. (2000). Shear behavior of clean rock joint. **Shear behavior of rock joints**.pp.17-51.

Jafari, M.K., Hosseini, K.A., Pellet, F., Boulon, M. and Buzzi, O. (2003). Evaluation of shear strength of rock joints subjected to cyclic loading. **Soil Dynamics and Earthquake Engineering** 23 (7): 619-630.

Jung-Wook Park, Jae-Joon Song. (2013). Numerical method for the determination of contact area of rock joints. **International Journal of Rock Mechanics & Mining Sciences** 58 (1): 8-22.

Kusumi, H., Teraoka, K., Nishida, K. (1997). Study on new formulation of shear strength for irregular rock joints. **International Journal of Rock Mechanics & Mining Sciences** 34 (3-4): 168.e1-168.e15.

Li B., Jing Y., Wang G. (2012). Evaluation of shear velocity dependency of rock fractures by using repeated shear tests. **Harmonising Rock Engineering and the Environment**. ISBN 978-0-415-80444-8.

Maksimovic, M. (1996). The shear strength components of a rough rock joint. **International Journal of Rock Mechanics and Mining Sciences & Geomechanics** Abstracts 33 (8): 769-783.

Ray, S. K., Srakar, M. and Singh, T. N. (1999). Effect of cyclic loading and strain rate on the mechanical behaviour of sandstone. **International Journal of Rock Mechanics and Mining Sciences** 36: 543-549.

Sangha, C. M. and Dhir, R. K. (1972). Influence of time on the strength, deformation and fracture properties of a lower Devonian sandstone. **International Journal of Rock Mechanics and Mining Sciences** 9: 343-354.

Seok-Won Lee, Eun-Soo Hong, Seok-Il Bae, In-Mo Lee. (2006). Modeling of rock joint shear strength using surface roughness parameter. **Tunneling and Underground Space Technology** 21: 239.

SONG Hongwei, DUAN Yanyan, YANG Jing. (2010). Numerical simulation on bolted rock joint shearing performance. **Mining Science and Technology** 20: 0460–0465.

Zhao, J. (1997). Joint surface matching and shear strength part b: JRC-JMC shear strength criterion. **International Journal of Rock Mechanics & Mining Sciences** 34 (2): 179-185.

BIOGRAPHY

Mr. Pinid Meemun was born on December 15, 1989 in Nongkhai province, Thailand. He received his Bachelor's Degree in Engineering (Geotechnology) from Suranaree University of Technology in 2011. For him post-graduate, he continued to study with a Master's degree in the Geological Engineering Program, Institute of Engineering, Suranaree university of Technology. During graduation, 2012-2014, he was a part time worker in position of research assistant at the Geomechanics Research Unit, Institute of Engineering, Suranaree University of Technology.